NATO Advanced Research Workshop

Metallic Materials with High Structural Efficiency

High Strength Microstructural Forms in Titanium Alloys Processed with Rapid Heat Treatment

Orest Ivasishin

G.V. Kurdyumov Institute for Metal Physics, Kyiv, Ukraine

Kiev, Ukraine

September 07-13, 2003

Report Documentation Page

Form Approved
OMB No. 0704-0188

1. REPORT DATE **18 MAR 2004**	2. REPORT TYPE **N/A**	3. DATES COVERED **-**
4. TITLE AND SUBTITLE **High Strength Microstructural Forms in Titanium Alloys Processed with Rapid Heat Treatment**		5a. CONTRACT NUMBER 5b. GRANT NUMBER 5c. PROGRAM ELEMENT NUMBER
6. AUTHOR(S)		5d. PROJECT NUMBER 5e. TASK NUMBER 5f. WORK UNIT NUMBER
7. PERFORMING ORGANIZATION NAME(S) AND ADDRESS(ES) **G.V. Kurdyumov Institute for Metal Physics, Kyiv, Ukraine**		8. PERFORMING ORGANIZATION REPORT NUMBER
9. SPONSORING/MONITORING AGENCY NAME(S) AND ADDRESS(ES)		10. SPONSOR/MONITOR'S ACRONYM(S) 11. SPONSOR/MONITOR'S REPORT NUMBER(S)

12. DISTRIBUTION/AVAILABILITY STATEMENT
Approved for public release, distribution unlimited

13. SUPPLEMENTARY NOTES
See also ADM001672., The original document contains color images.

14. ABSTRACT

15. SUBJECT TERMS

16. SECURITY CLASSIFICATION OF:			17. LIMITATION OF ABSTRACT	18. NUMBER OF PAGES	19a. NAME OF RESPONSIBLE PERSON
a. REPORT **NATO/unclassified**	b. ABSTRACT **unclassified**	c. THIS PAGE **unclassified**	**UU**	**73**	

Standard Form 298 (Rev. 8-98)
Prescribed by ANSI Std Z39-18

Outline

- Introduction:
  - Strengthening of titanium alloys
- Background of rapid heat treatment (RHT)
  - microchemical inhomogeneity
  - grain growth
- Examples of RHT:
  - alpha/beta alloys
  - beta alloys
- Super strength beta alloys
- Modulated structure of alpha double-prime martensite
- Texture Controlled Grain Growth Kinetics at Continuous Heating
- Conclusions

Specific Strength of Constructional Materials

NATO Advanced Research Workshop

Metallic Materials with High Structural Efficiency

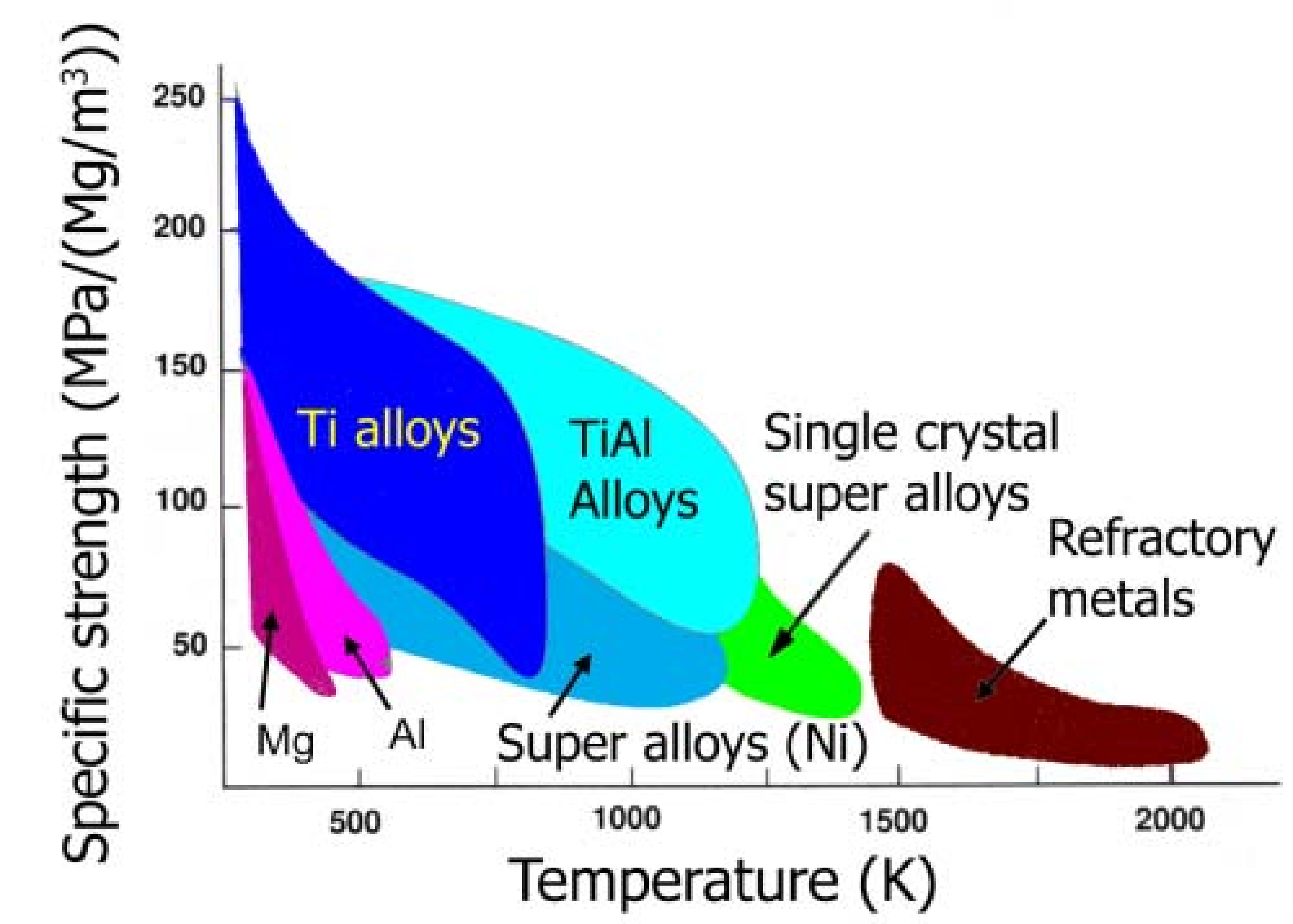

Property Requirements for Titanium Alloys in Aircraft Applications

NATO Advanced Research Workshop

Metallic Materials with High Structural Efficiency

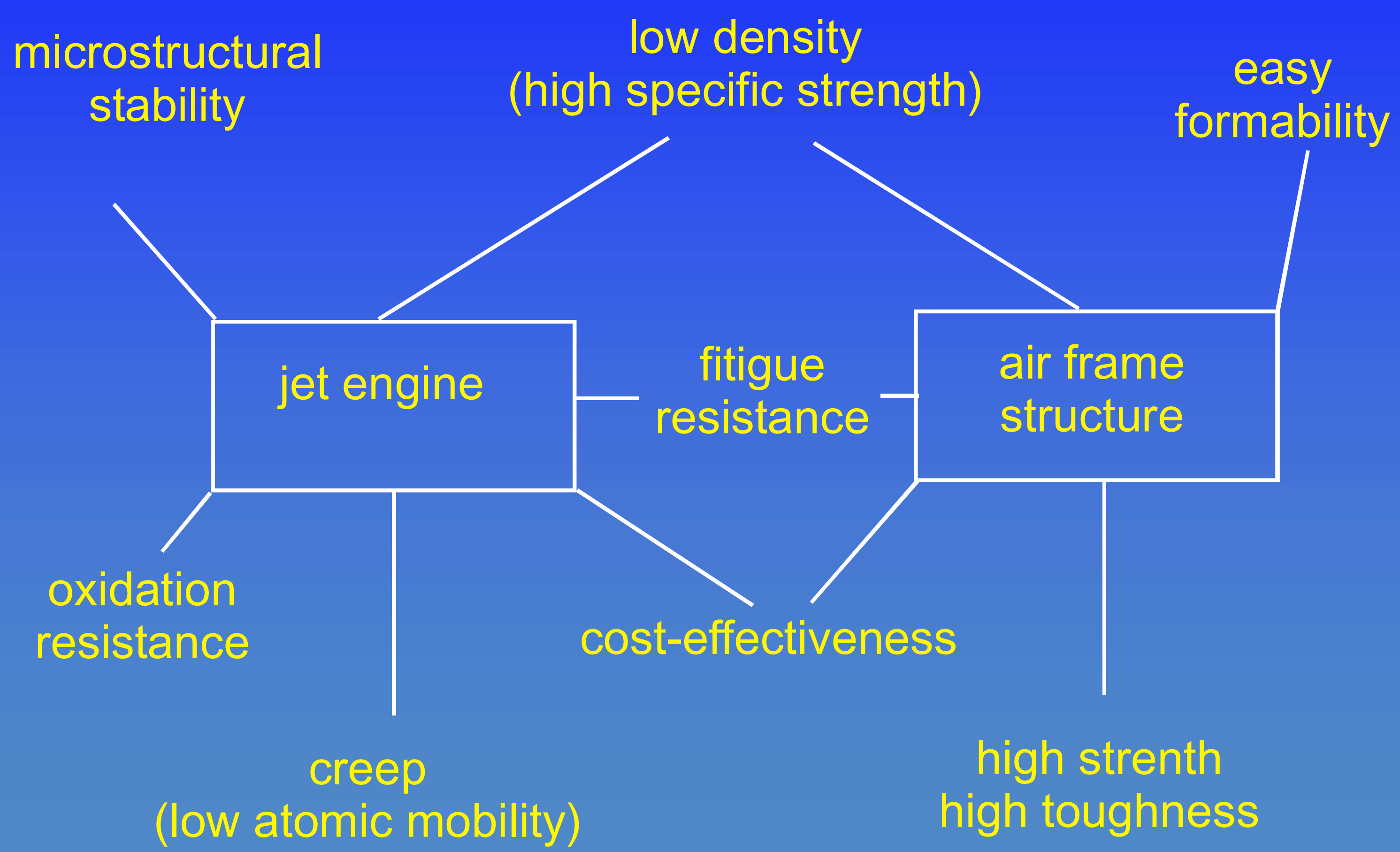

Strengthening Mechanisms of Titanium Alloys

1. Solid solutional (alloying of α-solid solution)

2. Textural

3. Dispersional

4. Heterogeneous (α(h.c.p.)<->β(b.c.c.) phase transformation)

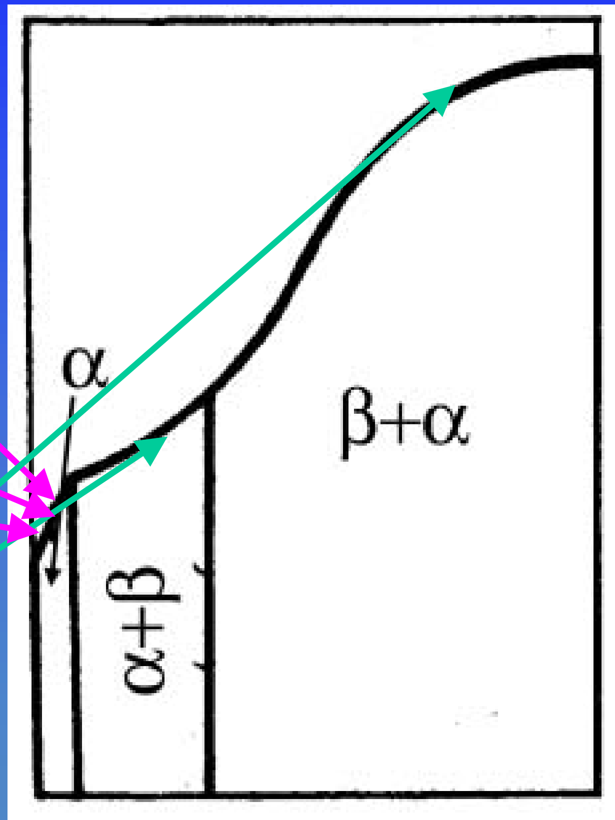

Heat Treatment

NATO Advanced Research Workshop
Metallic Materials with High Structural Efficiency

$\alpha'_{met}(\alpha'') \rightarrow \alpha+\beta$

$\beta_{met} \rightarrow \alpha+\beta$

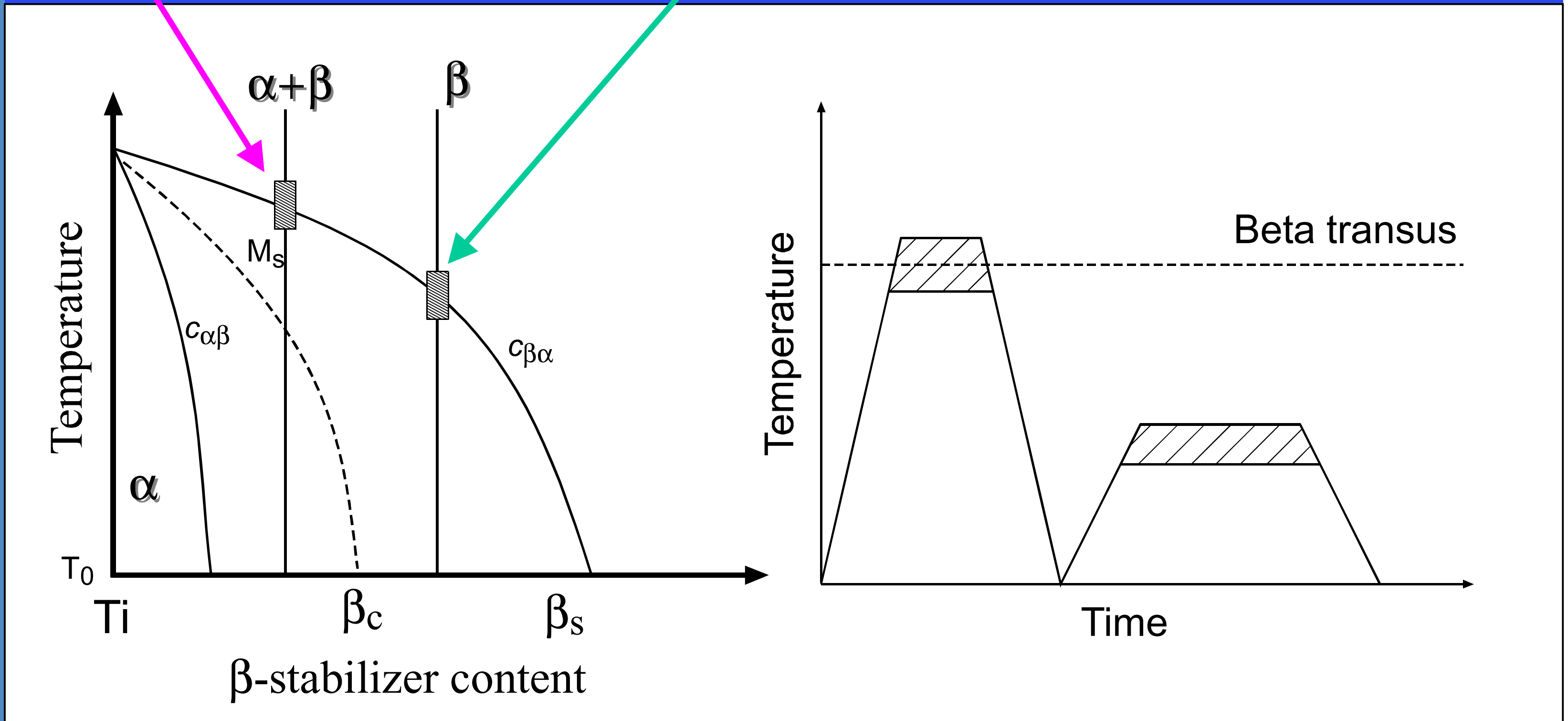

Grain Size Dependence of Ductility (scheme)

NATO Advanced Research Workshop

Metallic Materials with High Structural Efficiency

YS1

YS2

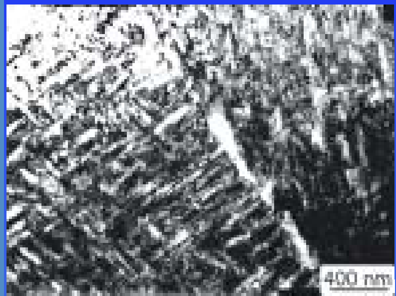

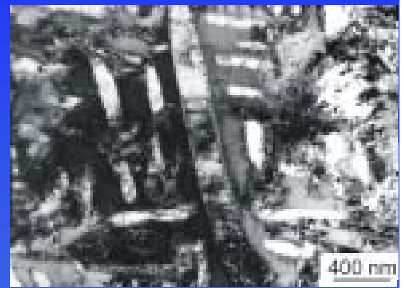

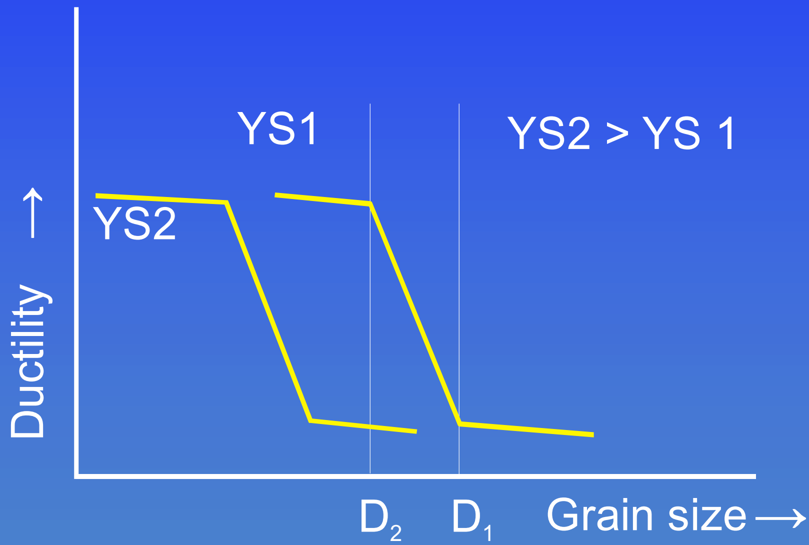

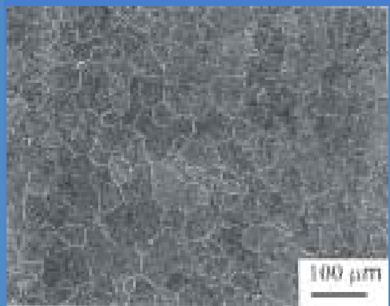

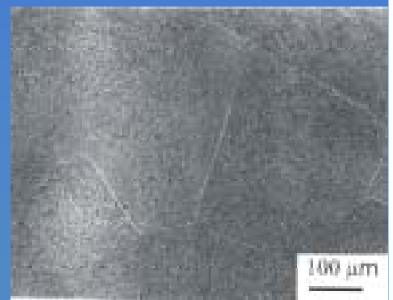

Conventional Heat Treatment

NATO Advanced Research Workshop
Metallic Materials with High Structural Efficiency

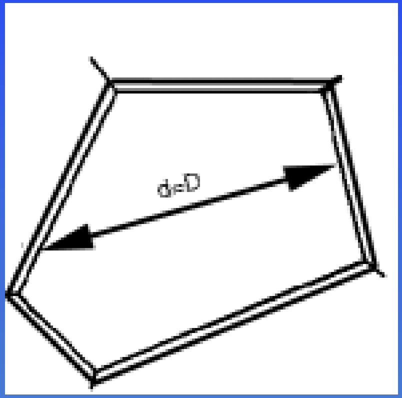

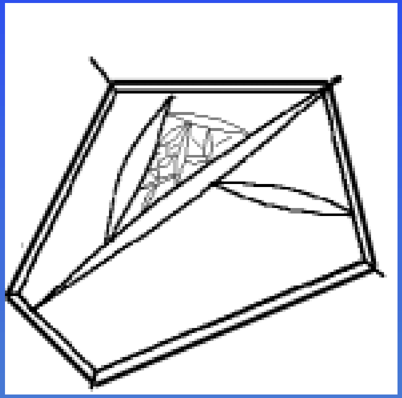

Compromise: Bimodal Microstructures

NATO Advanced Research Workshop
Metallic Materials with High Structural Efficiency

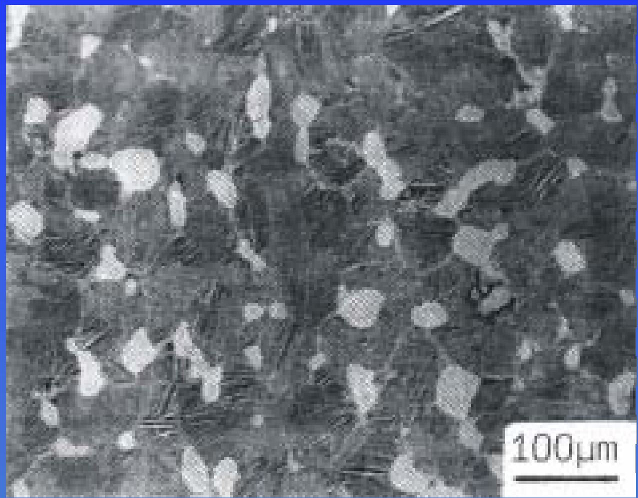

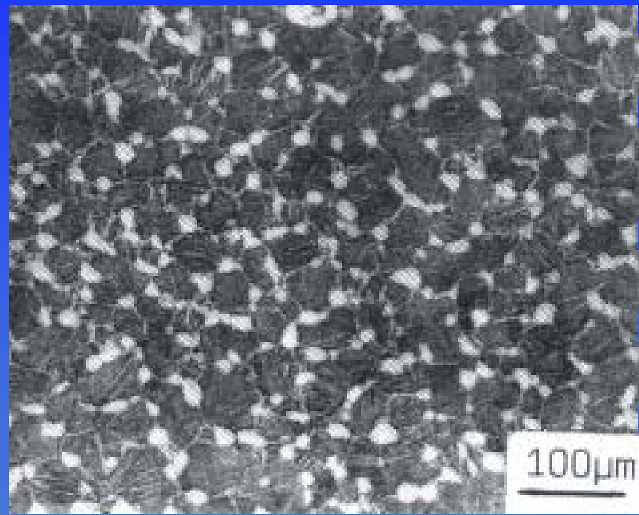

- sensitive to α_{pr} volume fraction and size due to:
  - partitioning effect;
  - α_{pr} texture.
- therefore needs very careful processing

Background of Rapid Heat Treatment (RHT)

RHT Background

TECHNICAL ESSENCE:

- rapid continuous heating above β-transus followed by instantaneous cooling; Controlled parameters:
  - heating rate;
  - peak temperature;
  - cooling rate;

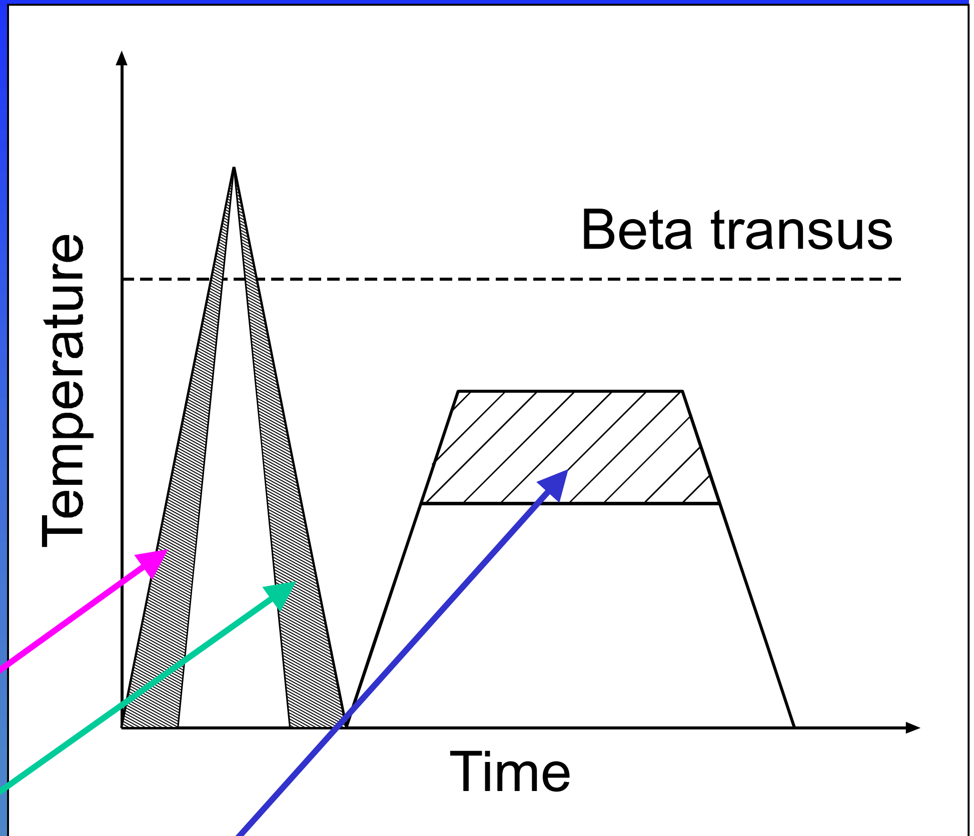

rapid heating — cooling — aging

$\alpha+\beta \rightarrow \beta \rightarrow \alpha'+\alpha''+\beta_{met} \rightarrow a+\beta$

RHT Background

MICROSTRUCTURAL FEATURES:

- full dissolution of primary a;
- small beta-grain sizes;
- fine lamellar/acicular intragrain microstructure formed through:
  - •in $\alpha+\beta$ alloys:
    - •martensite type transformation
    - •diffusion controlled transformation
  - •in β alloys:
    - •precipitation hardening

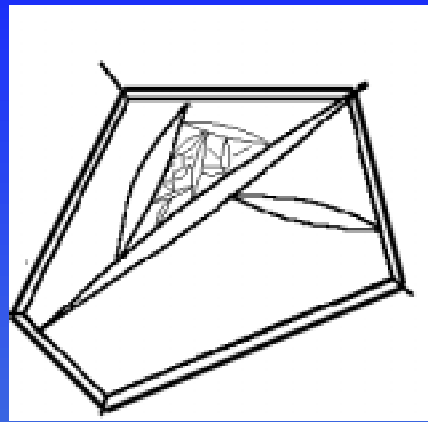

Conventional heat treatment

RHT

Fine-Grained and Coarse-Grained Microstructures

NATO Advanced Research Workshop

Metallic Materials with High Structural Efficiency

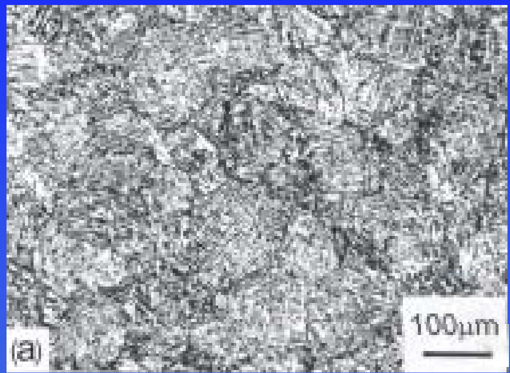

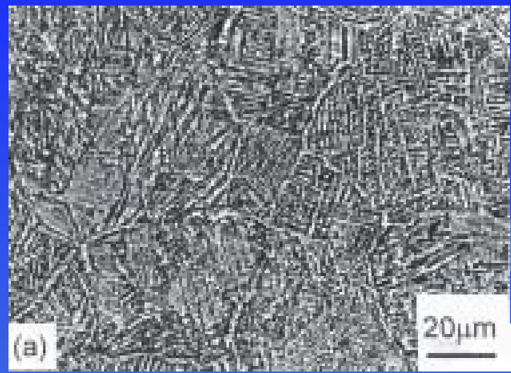

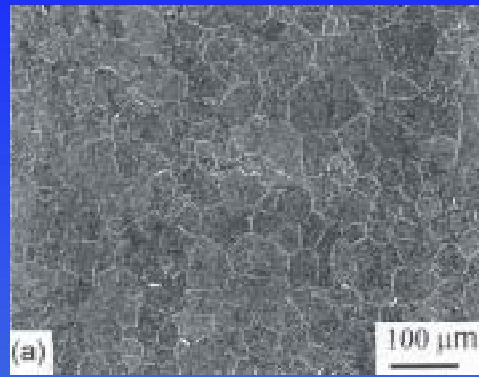

VT18Y | VT6 | β-CEZ

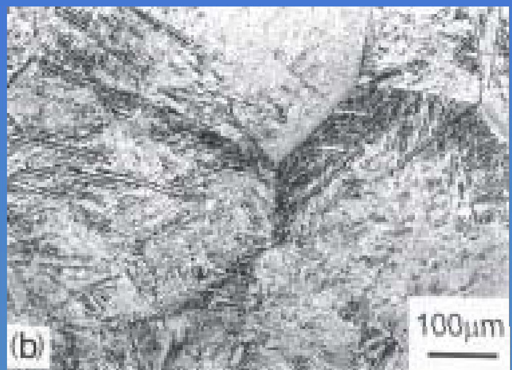

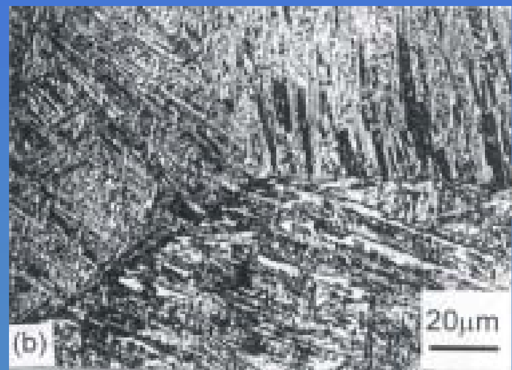

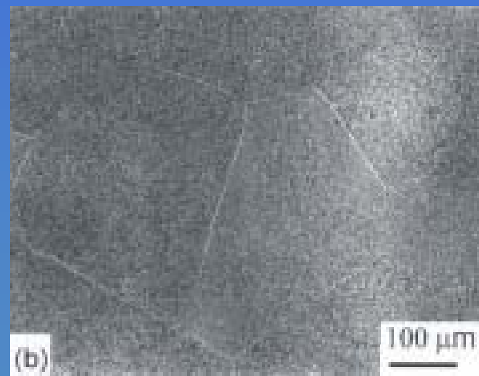

Grain Structure Evolution on Heating

Isothermal conditions:

$$D^n - D_0^n = Kt\exp\left(-Q/RT\right)$$

Continuous heating

$$D^n - D_0^n = \left(KR/\dot{T}Q\right)\left\{\left[T_f^2\exp\left(-Q/RT_f\right)\right]-\left[T_i^2\exp\left(-Q/RT_i\right)\right]\right\}$$

Isotropic condition

Textured condition

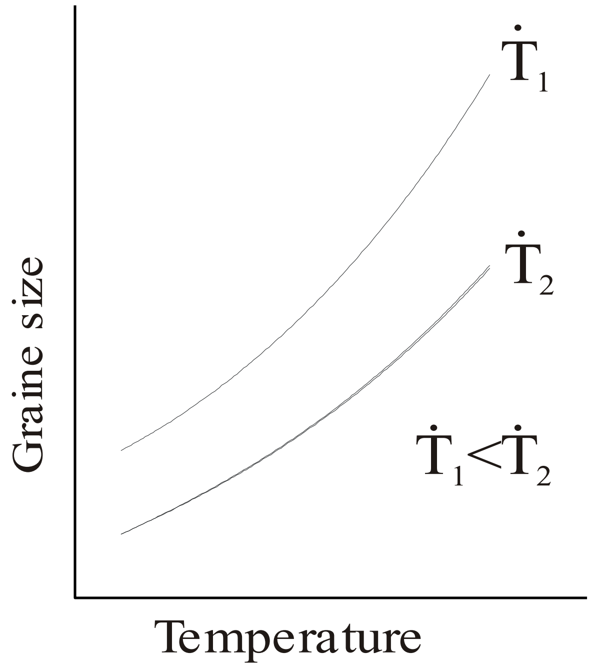

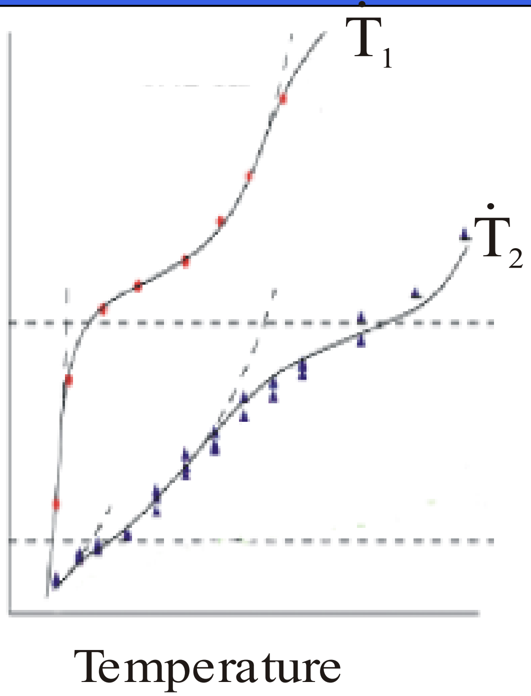

Microchemical Inhomogeneity

NATO Advanced Research Workshop
Metallic Materials with High Structural Efficiency

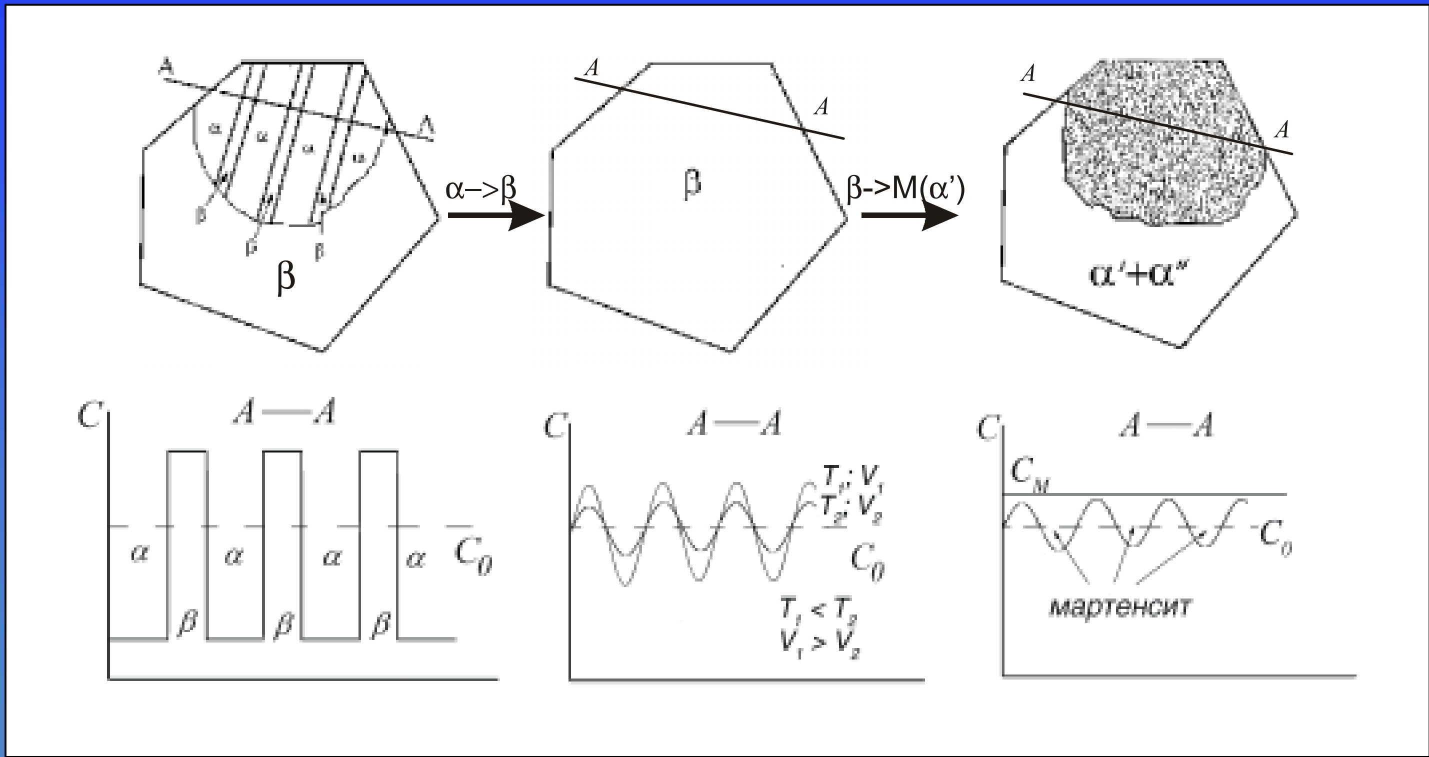

Microchemical Inhomogeneity

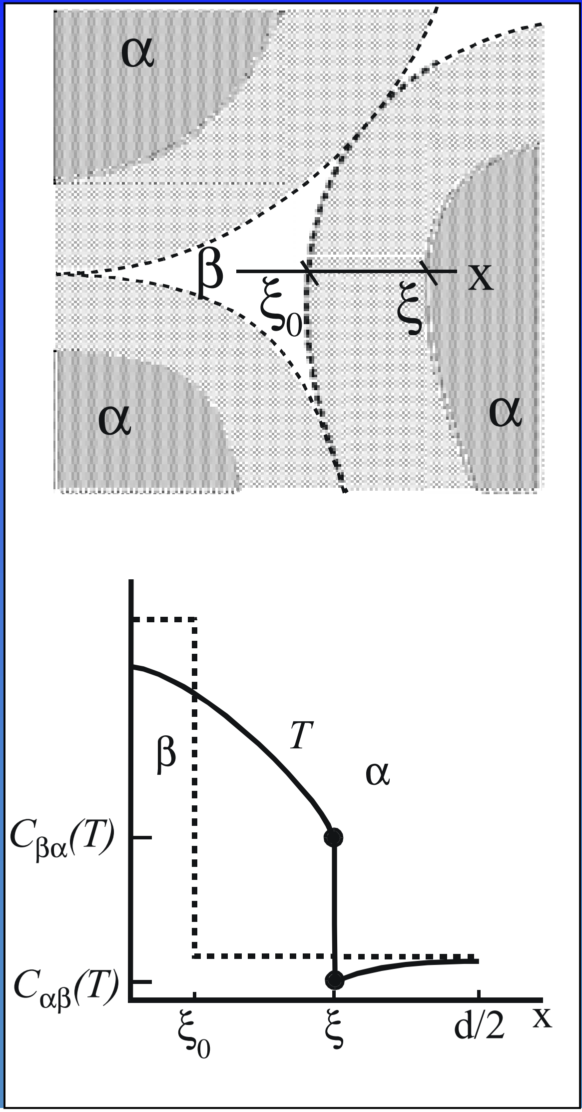

$$(C_{\beta\alpha} - C_{\alpha\beta})\frac{d\xi}{dT}\dot{T} = -D_\alpha(T)\frac{\partial C_\alpha}{\partial x}\Big|_{x=\xi^+} + D_\beta(T)\frac{\partial C_\beta}{\partial x}\Big|_{x=\xi^-}$$

$$\frac{\partial C_\beta}{\partial T} = \frac{1}{\dot{T}} D_\beta(T)\frac{\partial^2 C_\beta}{\partial x^2}; \qquad 0 \le x \le \xi$$

$$\frac{\partial C_\alpha}{\partial T} = \frac{1}{\dot{T}} D_\alpha(T)\frac{\partial^2 C_\alpha}{\partial x^2}; \qquad \xi \le x \le \frac{d}{2}$$

Starting conditions:

$$C_\alpha(x, T_0) = C_{\alpha_0}; \qquad C_\beta(x, T_0) = C_{\beta_0}$$

Boundary conditions:

$$C_\alpha(\xi, T) = C_{\alpha\beta}(T); \qquad C_\beta(\xi, T) = C_{\beta\alpha}(T)$$

$$\frac{\partial C_\alpha}{\partial x}\Big|_{x=d/2} = \frac{\partial C_\beta}{\partial x}\Big|_{x=0} = 0$$

Microchemical Inhomogeneity in VT23 Alloy (STEM)

NATO Advanced Research Workshop
Metallic Materials with High Structural Efficiency

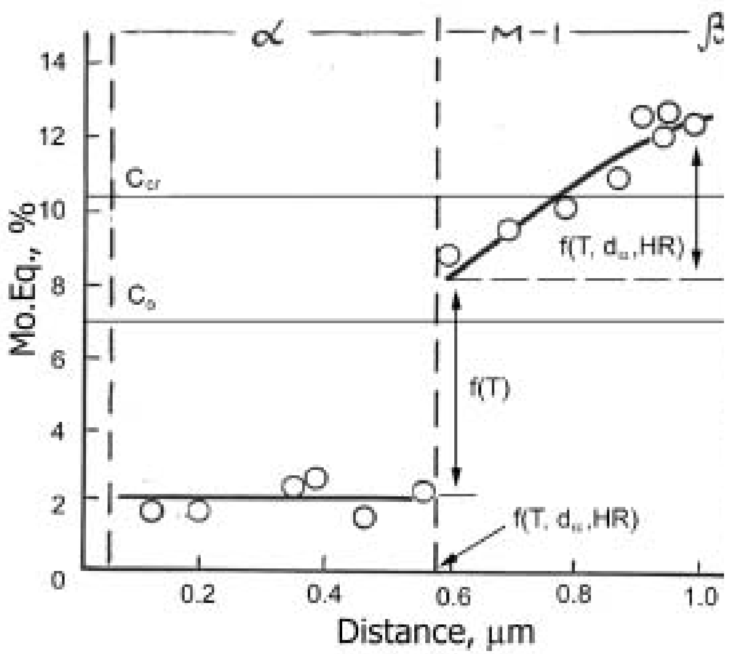

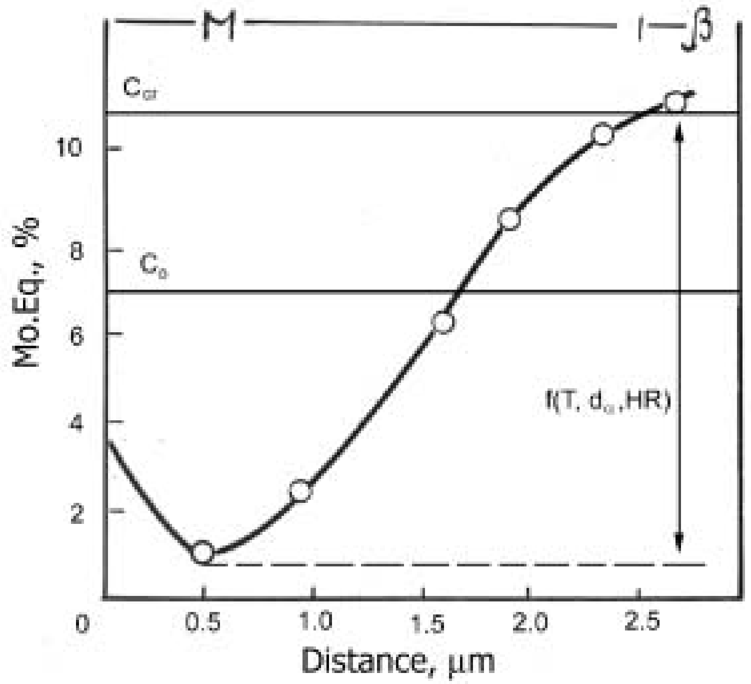

α+β ST

β ST

NATO Advanced Research Workshop

Metallic Materials with High Structural Efficiency

Strength

$$\sigma=\sigma_0+kd^{-1/2}$$

Unfragmented grain	Fragmentation in homogeneous phase	Fragmentation using volume concentrational modulation

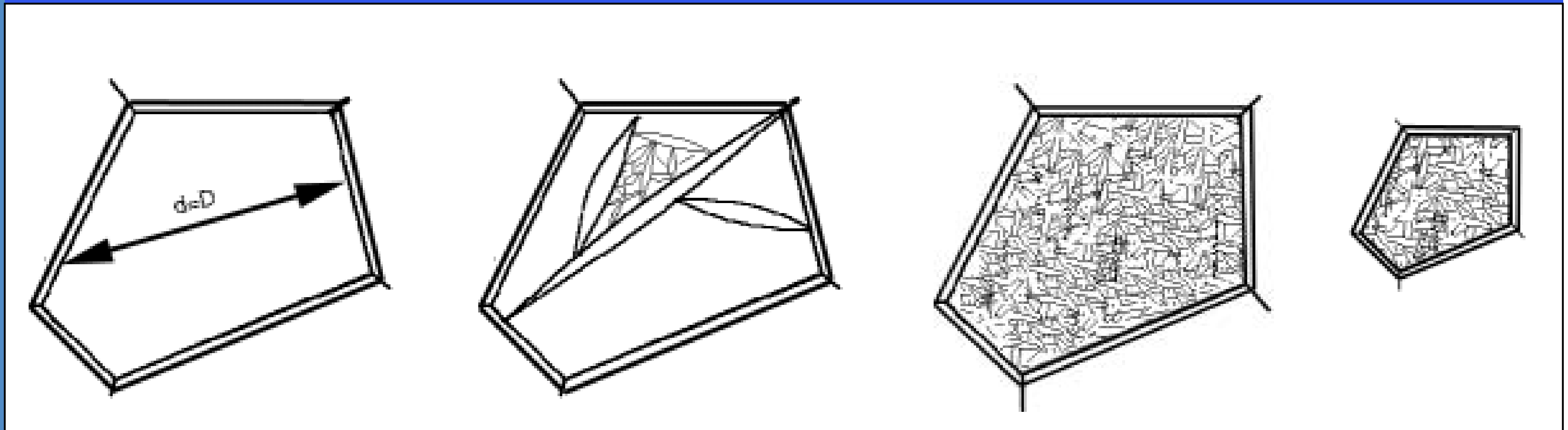

d=D≅100 μm	d≅1–10 μm	d≅0.05–0.5 μm	
	D≅100 μm	D≅100 μm	D≅10 μm

Examples of RHT

Strength/Ductility Relationship in $\alpha+\beta$ Alloys

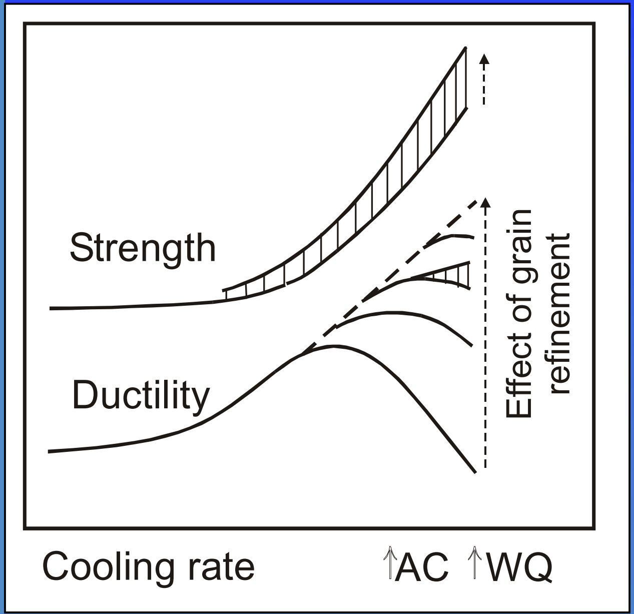

Ti-6Al-4V; WQ

grain size 500 mm: YS = 1105 MPa; A5 = 4.6%;

grain size 80 mm: YS = 1105 MPa; A5 = 9.9%;

grain size 30-50 mm: YS = 1268 MPa; UTS = 1349 MPa; A5 = 10.9%

VT23 (Ti-0.5Al-2.0Mo-4.5V-1Cr-1Fe);WQ

grain size 300 mm: UTS = 1350 MPa; A5 = 1%;

grain size 20 mm: UTS = 1900 MPa; A5 = 6%;

Microchemical Inhomogeneity of β-Phase

NATO Advanced Research Workshop

Metallic Materials with High Structural Efficiency

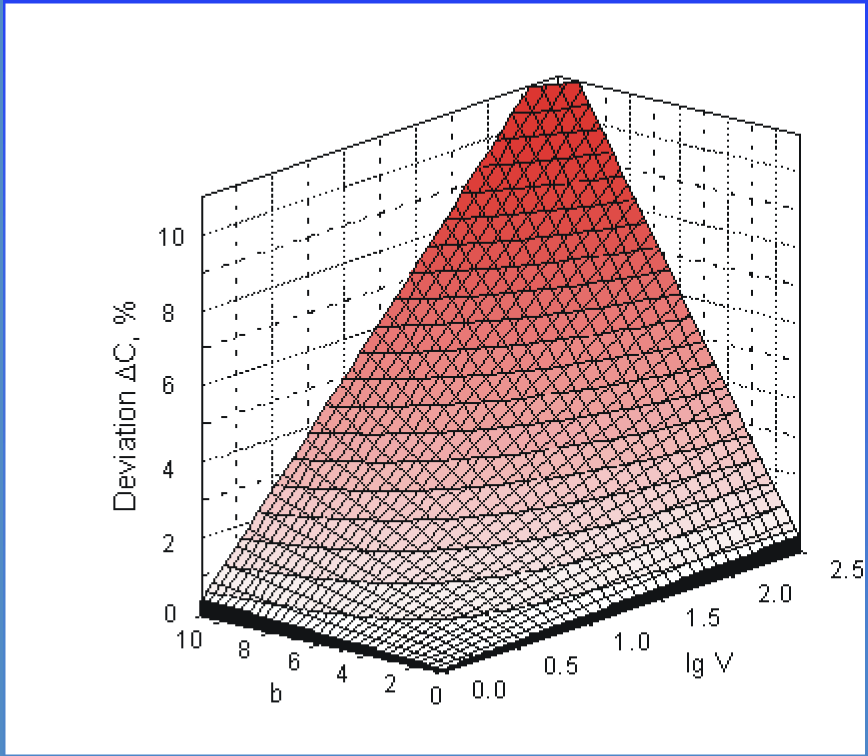

$$\Delta C = f\left(C_0, d, \dot{T}, T_p\right)$$

For $C_0 = const; \quad T = T_\beta$

$$\Delta C = f\left(d, \dot{T}\right)$$

Ti-6Al-4V; C_0=2.66

S-N Curves of Ti-6Al-4V

NATO Advanced Research Workshop
Metallic Materials with High Structural Efficiency

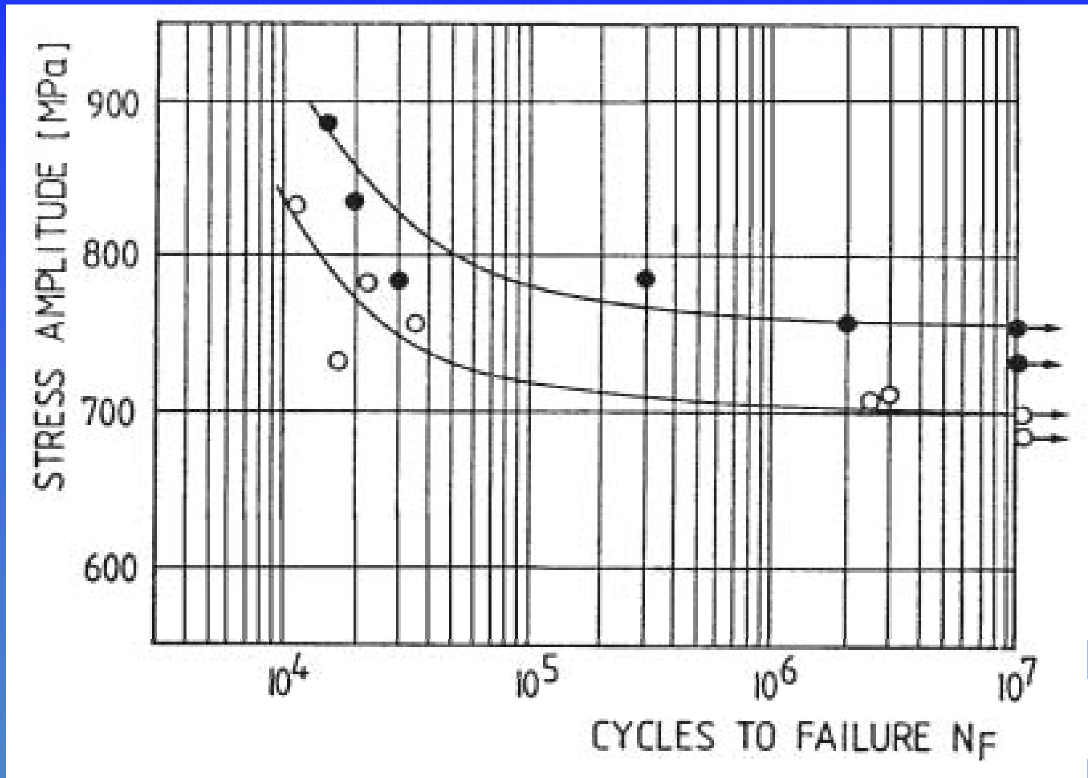

open symbols - coarse-grained
closed symbols - fine-grained

Fatigue Crack Nucleation Sites

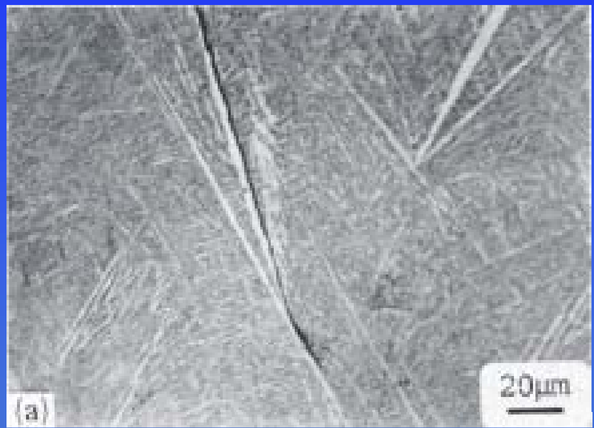

FH-WQ

RH-WQ

Ti 6242

Fatigue Microcrack Propagation in Fine-Grained Ti-6Al-4V

Beta-Transformed (Diffusion-Controlled) Fine-Grained Microstructures

NATO Advanced Research Workshop

Metallic Materials with High Structural Efficiency

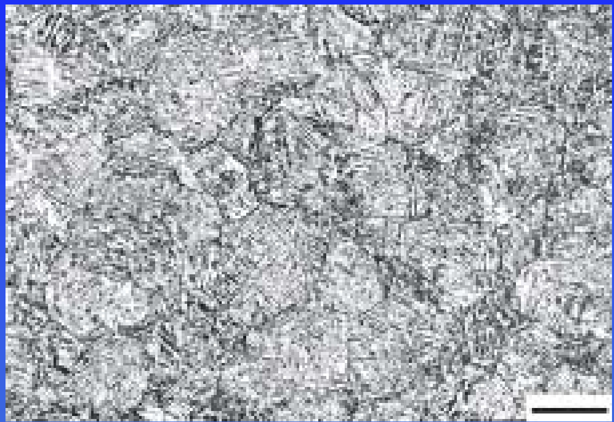

100µm

Alloy	Condition	A_5,%
Ti-6Al-4V	LG/AC	7.6
	FG/AC	11.4
Ti6242	LG/AC	6.1
	FG/AC	11.2
IMI 834	LG/AC	5.2
	FG/AC	14.4

100µm

Ti6242

Condition	$\sigma_{0.2}$, MPa	UTS, MPa	A_5, %	ε_F	$\varepsilon_{pl.}$, %	σ_{max} 10^7, MPa	σ_{max} 10^4, MPa
FG/AC	930	1065	11	0.40	0.12	525	750
Bi-modal	945	1055	12	0.47	0.15	500	675

Ductility of High Strength Beta Alloys as a Function of Beta-Grain Size

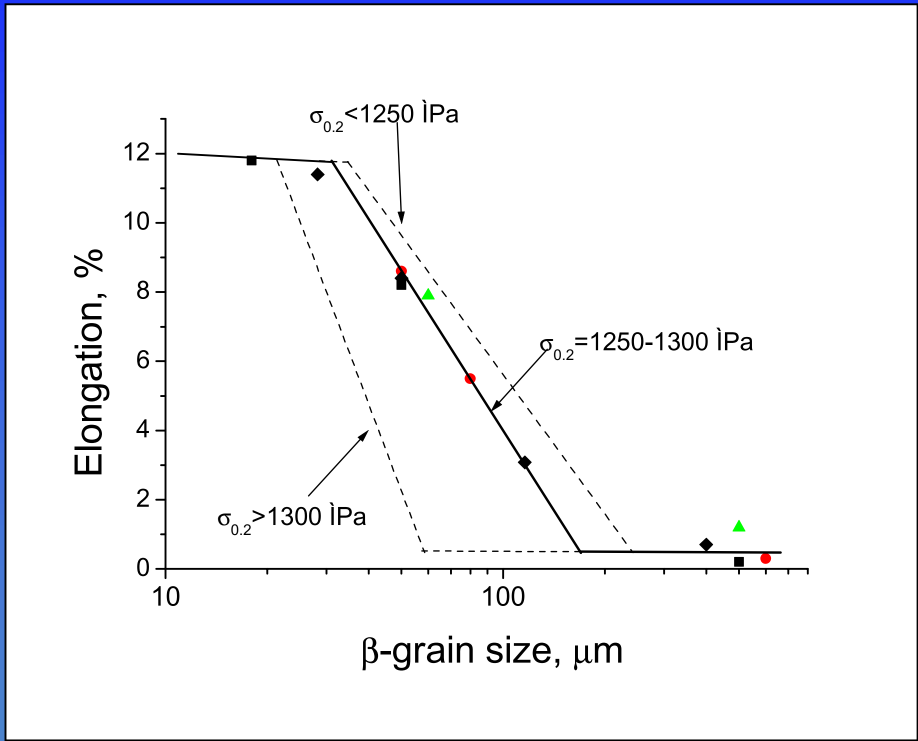

S-N Curves of β-CEZ and VT22

NATO Advanced Research Workshop

Metallic Materials with High Structural Efficiency

room temperature, R=-1, 50 Hz

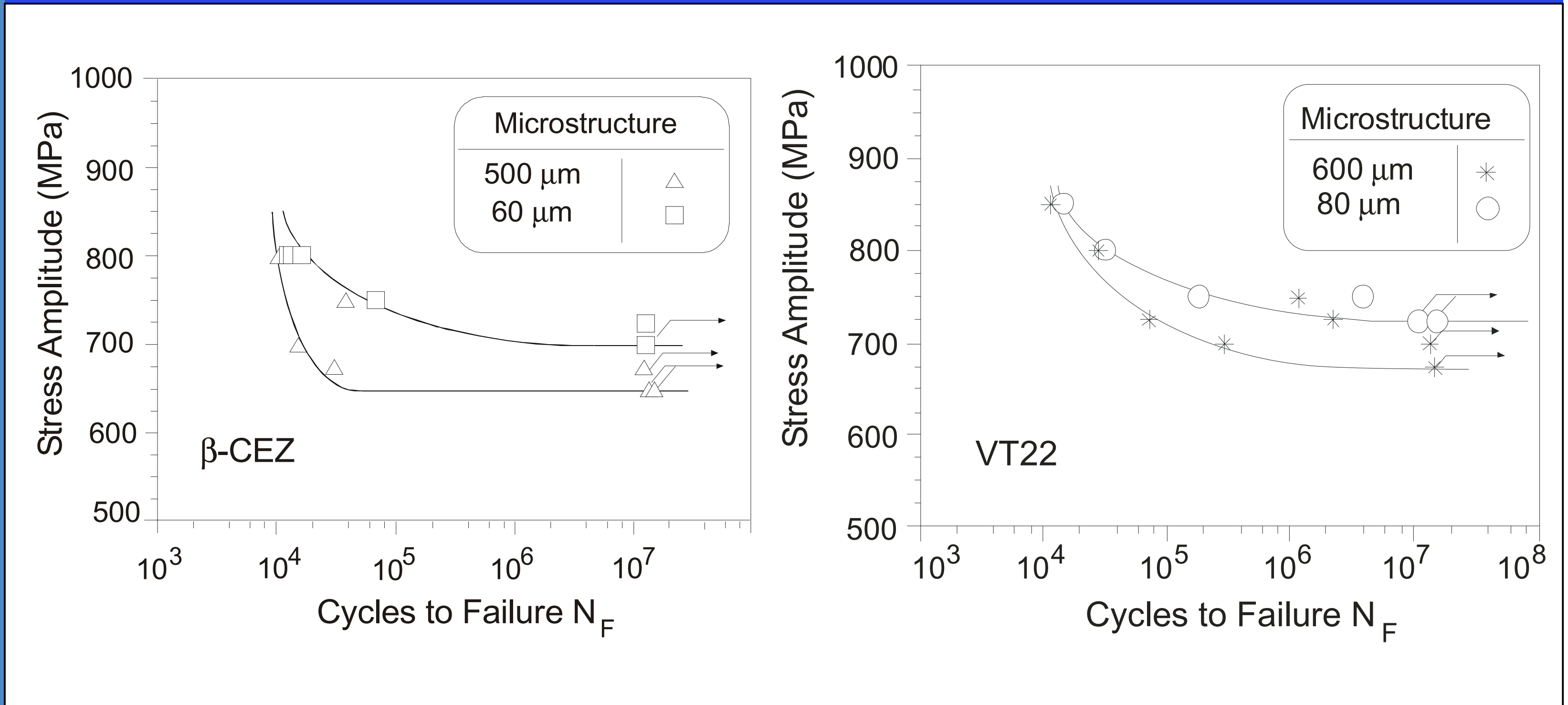

Fatigue Microcracks in β-CEZ

NATO Advanced Research Workshop
Metallic Materials with High Structural Efficiency

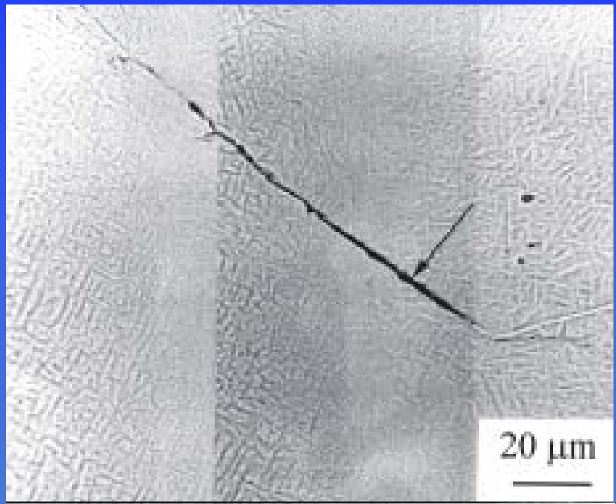

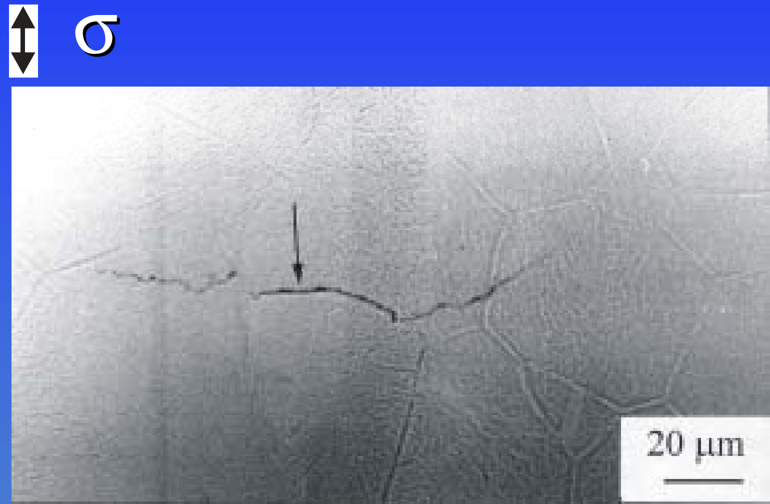

coarse-grained

fine-grained

Micro- and Macrocrack Propagation in β-CEZ

NATO Advanced Research Workshop
Metallic Materials with High Structural Efficiency

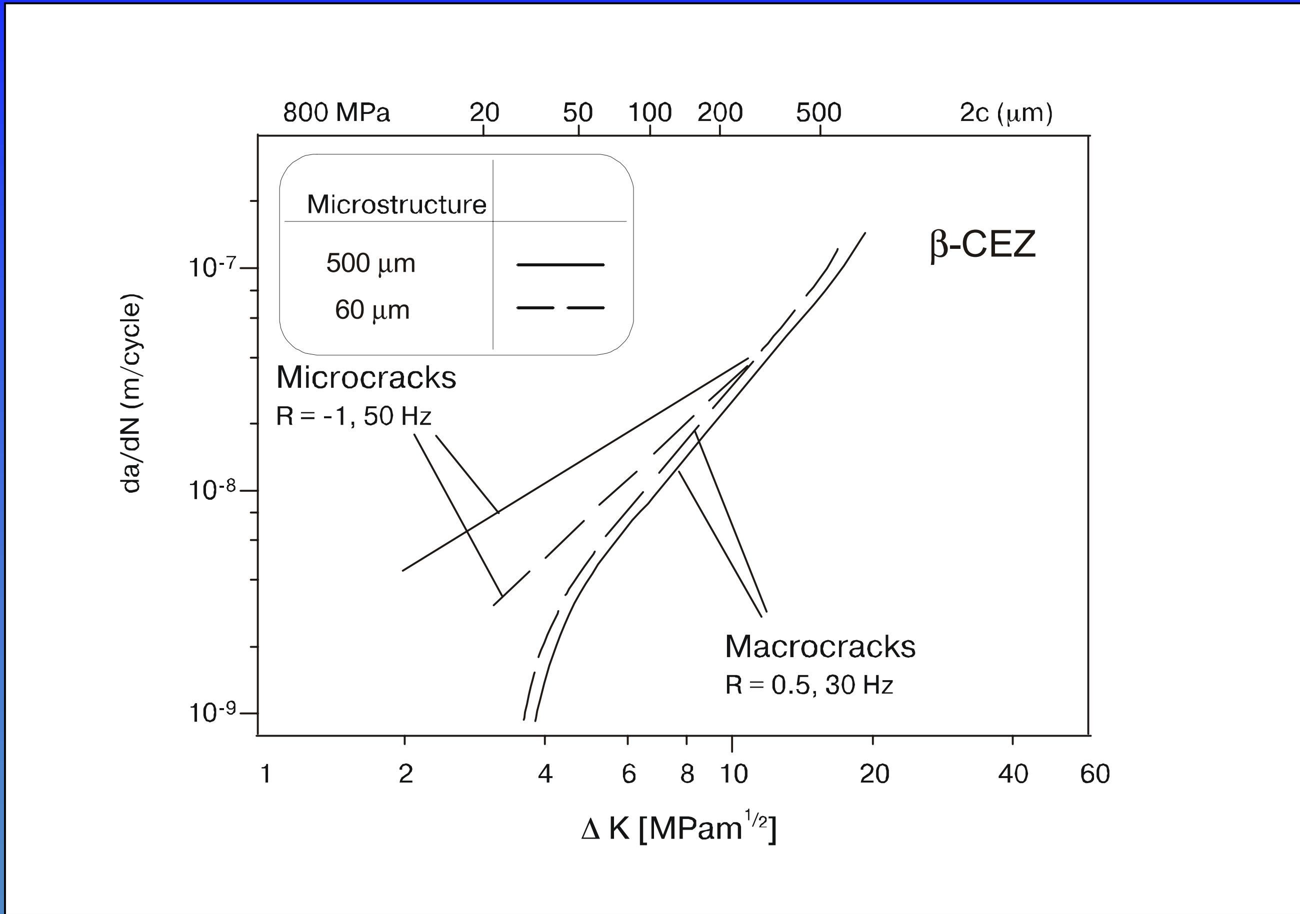

NATO Advanced Research Workshop

Metallic Materials with High Structural Efficiency

Super Strength Beta Alloys

Critical Grain Sizes as a Function of Strength

NATO Advanced Research Workshop
Metallic Materials with High Structural Efficiency

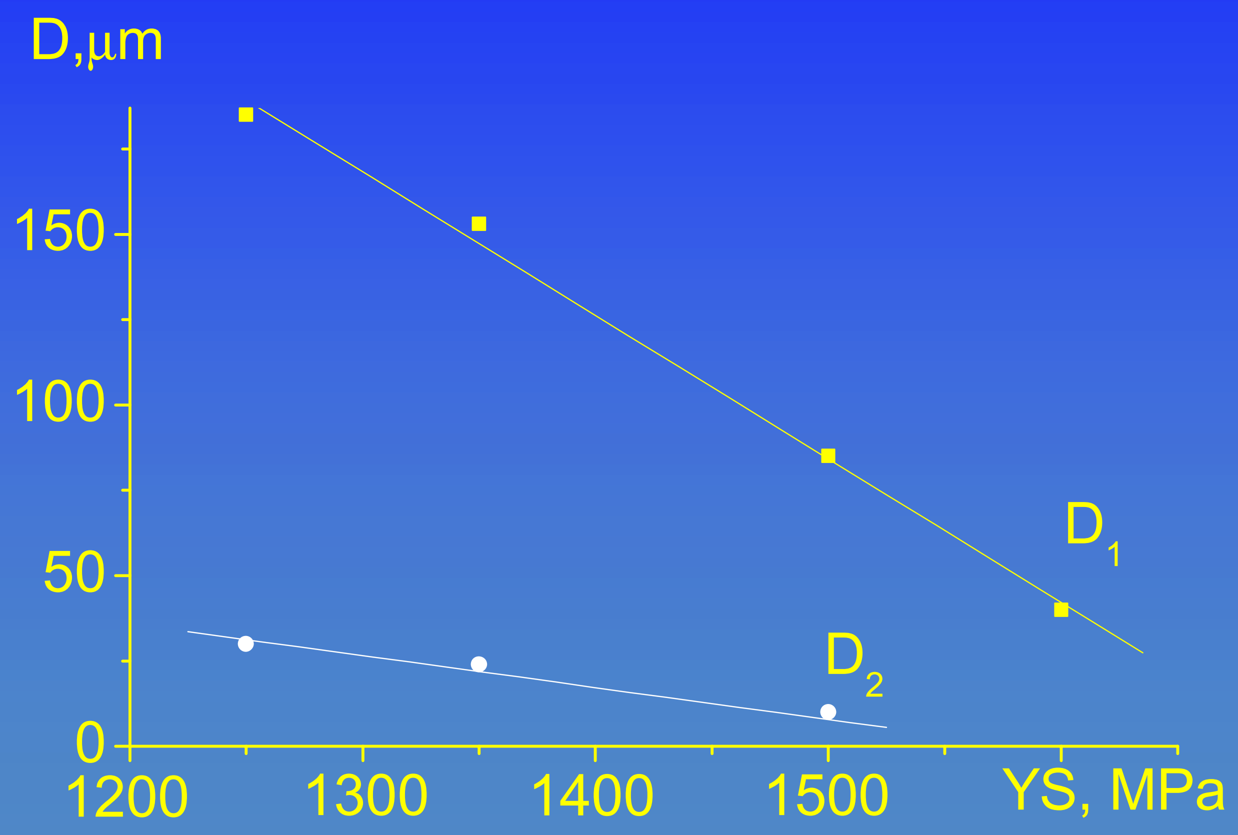

Coil Spring

$$\text{Volume} = \frac{G}{\tau^2}\left[2P^2/R\right]$$

$$\text{Weight} = \frac{G\rho}{\tau^2}\left[2P^2/R\right]$$

G – shear modulus
ρ – density
τ – shear stress
R – spring rate
P – load

Titanium advantage as compared to steels:

-25 % in volume

-2 to 1 in weight

Cold Deformation in Thermal Strengthening

The introduction of cold deformation between solution treatment and aging may have a beneficial effect on the evolution of microstructure because dislocations and other defects can modify the nucleation of alpha precipitates.

Additional recrystallization heat treatment results in a finer grain microstructure that yields a better balance of strength and ductility.

The best way to control beta grain size during recrystallization is through the use of continuous, rather than isothermal, heat treatment.

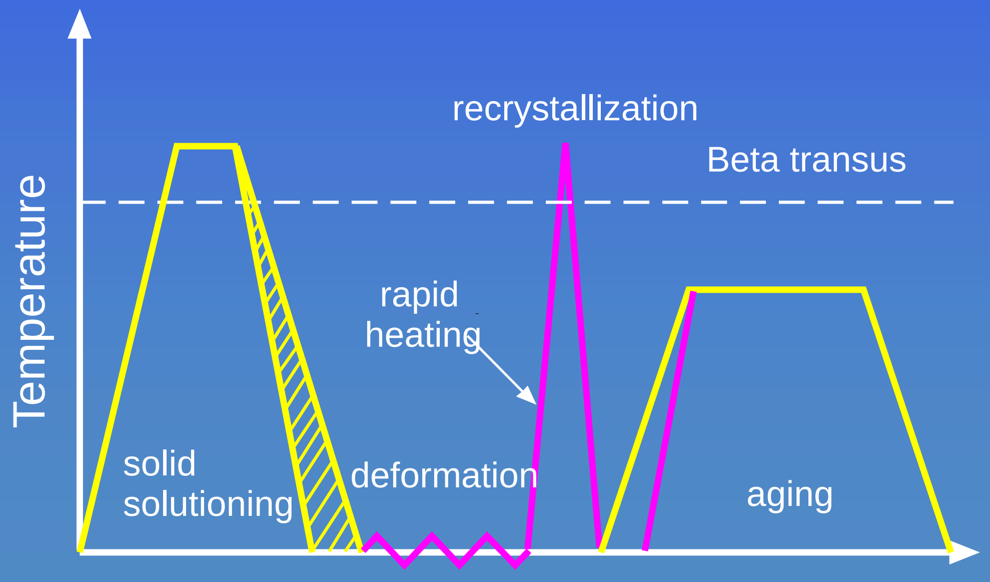

NATO Advanced Research Workshop
Metallic Materials with High Structural Efficiency

Program Alloys

Alloy	Composition (wt. pct.)						Mo. Eq.	Beta Transus (^{o}C)
	Al	Sn	Mo	V	Fe	Cr		
VT22	5.0	-	4.8	4.7	0.97	0.71	7.0	850
Ti-15-3	2.8	2.9	-	15.5	-	3.15	12.6	760
TIMETAL -LCB	1.5	-	6.8	-	4.5	-	18.4	790

Three commercial beta titanium alloys with different amounts of beta-stabilizing elements were used in the present program.

Recrystallization Behavior

Continuous Heating at 5 Ks^{-1}

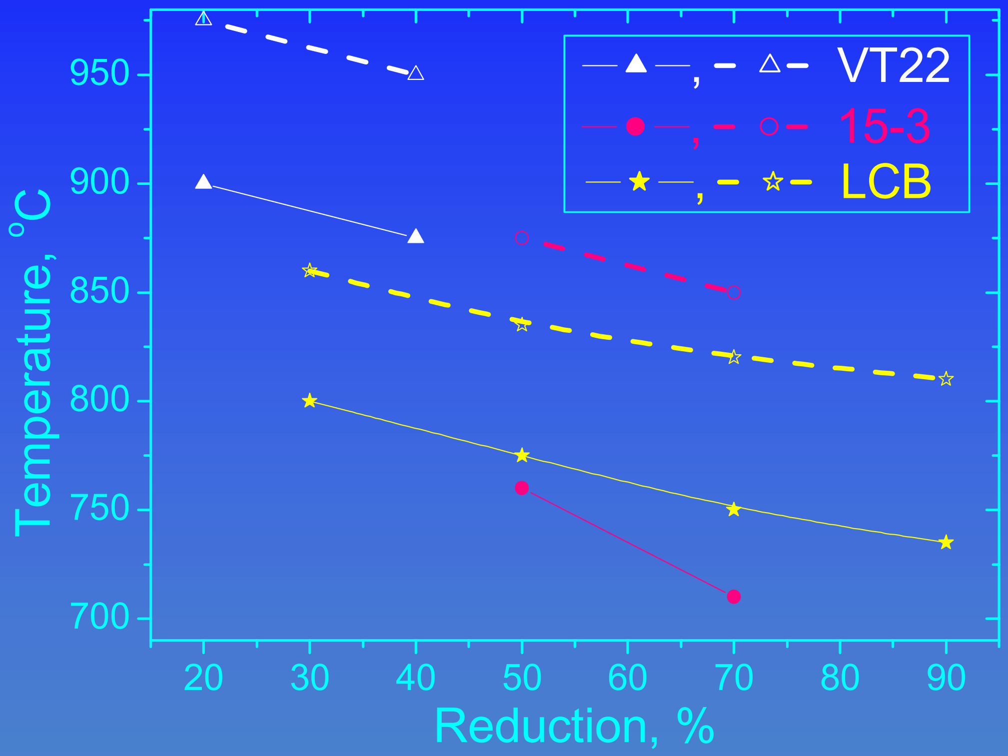

Closed and open symbols correspond to the start and finish of recrystallization, respectively

TIMETAL-LCB recrystallized more readily than Ti-15-3. The recrystallization interval was narrower and the recrystallization *finish* temperatures were lower for TIMETAL-LCB.

NATO Advanced Research Workshop

Metallic Materials with High Structural Efficiency

NATO Advanced Research Workshop
Metallic Materials with High Structural Efficiency

Recrystallization Behavior

Continuous Heating at 5 Ks^{-1}

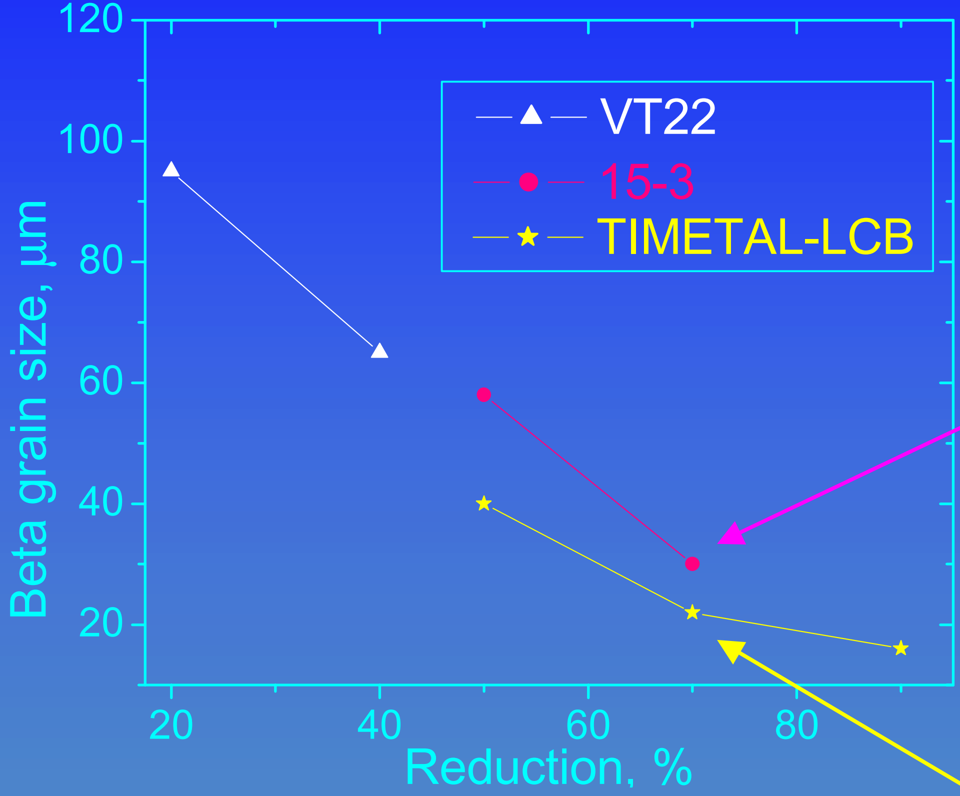

The narrower recrystallization interval and the lower recrystallization *finish* temperature led to a finer beta-grain size in TIMETAL-LCB for a given set of processing parameters.

Example:
70 pct. Reduction +
Continuous Heating

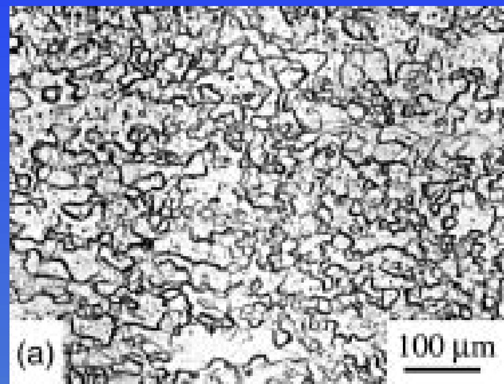

Ti-15-3

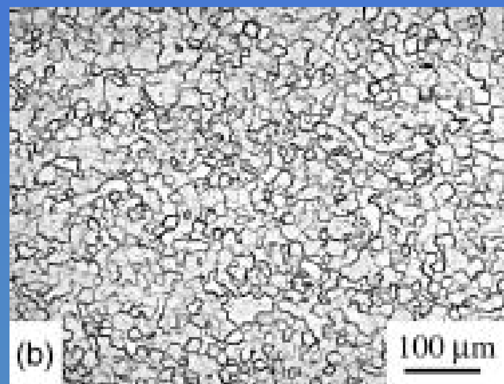

TIMETAL-LCB

NATO Advanced Research Workshop

Metallic Materials with High Structural Efficiency

Aging Response

Microstructure

Ti-15-3 after aging at 560ºC for 8 h

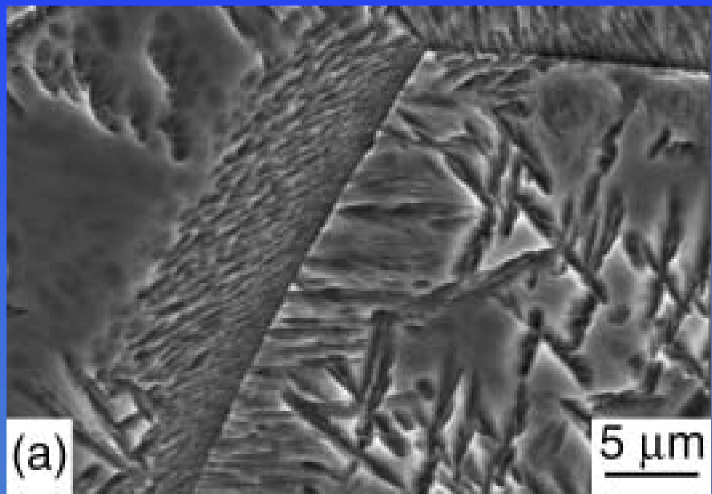

Coarse-grained

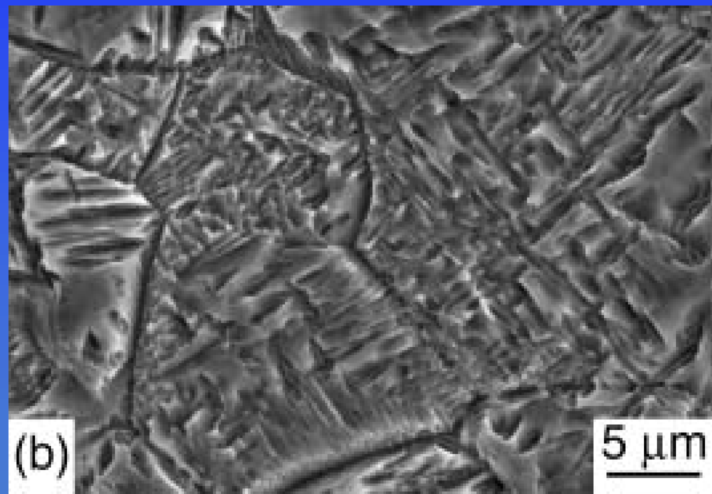

Fine-grained

Alpha precipitation began earlier in samples with smaller beta grains and resulted in larger amounts of precipitate and noticeably fewer precipitate-free zones.

Intragrain Microstructure in TIMETAL®-LCB

NATO Advanced Research Workshop
Metallic Materials with High Structural Efficiency

Influence of aging time, T=560°C

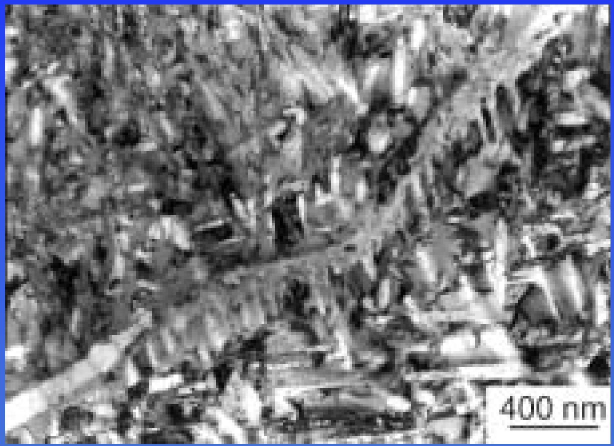

2 h

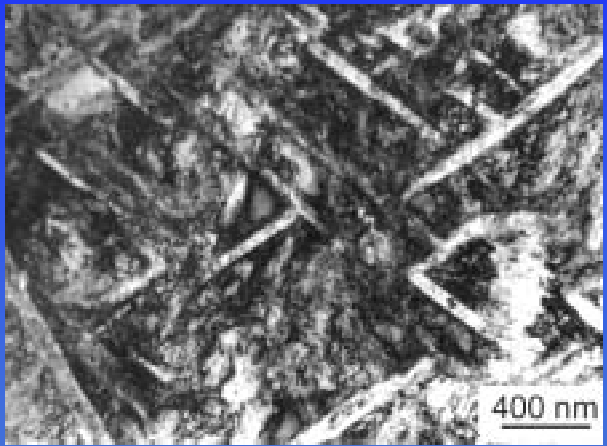

4 h

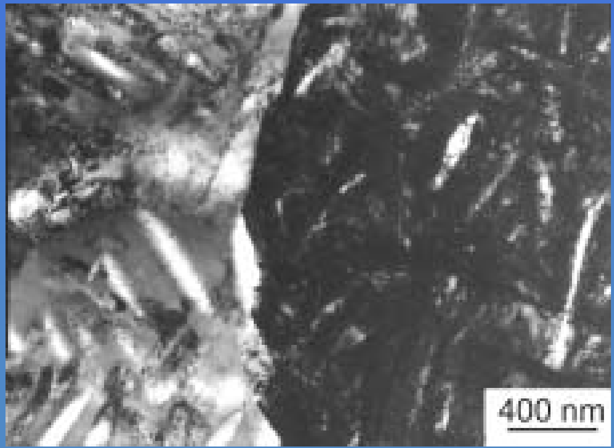

8 h

Intragrain Microstructure in TIMETAL®-LCB

NATO Advanced Research Workshop

Metallic Materials with High Structural Efficiency

Influence of aging temperature, t=8 h

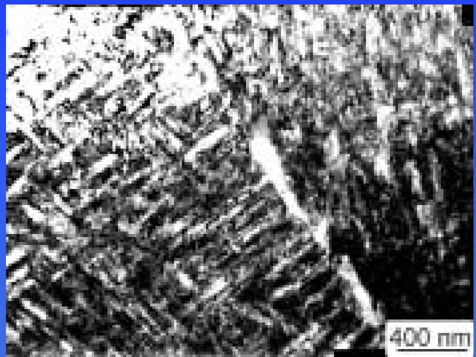

538 ^{o}C

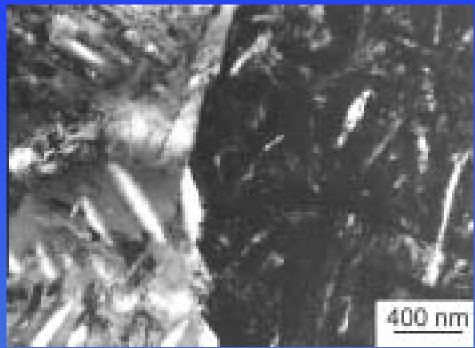

560 ^{o}C

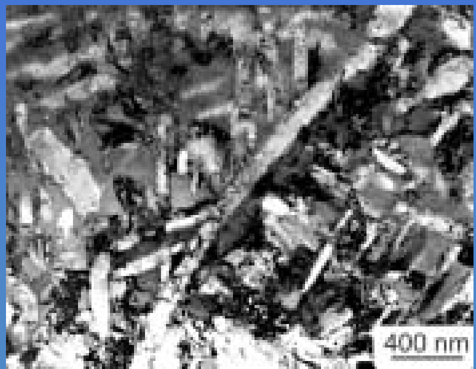

580 ^{o}C

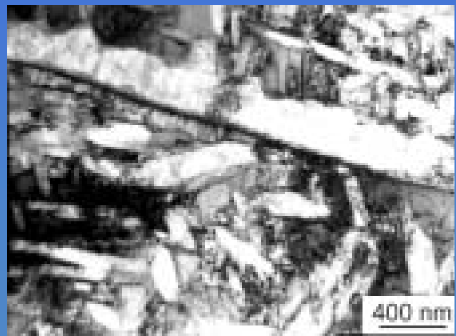

600 ^{o}C

Mechanical Properties of LCB: Influence of Grain Size

##	Solid solutioning	Grain size, µm	Reduc-tion, %	Recrysta-llization	Grain size, µm	YS, MPa	UTS, MPa	A_5,%	RA,%
1	β-furnace	90	–	–	*90*	1210	1210	brittle failure	
2	β-furnace	90	50	RRA	*30*	1395	1425	6.8	24
3	β-rapid heating	20	–	–	*17*	1450	1460	5.0	19
4	β-rapid heating	20	50	RRA	*12*	1420	1470	8.2	22.5
5	β-rapid heating	20	70	RRA	*7*	1475	1490	10.3	25.5

Aging: 538 °C, 8h

NATO Advanced Research Workshop

Metallic Materials with High Structural Efficiency

Aging Response

Influence of Heating Rate

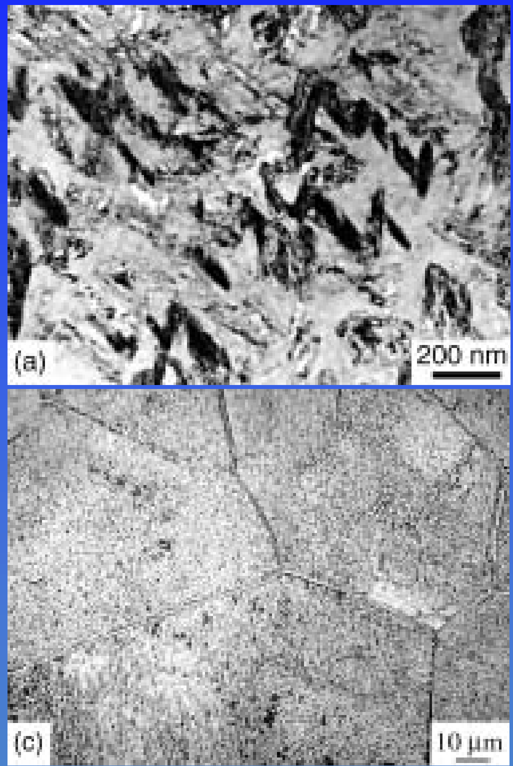

TIMETAL-LCB

538ºC, 2 h

676 ºC, 75 min

0.033 Ks^{-1} 20 Ks^{-1}

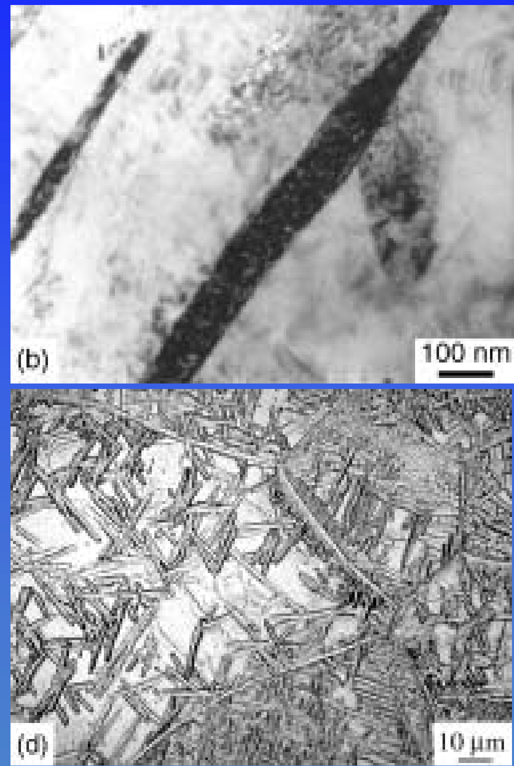

With slow heating, omega precipitation preceded nucleation of the alpha phase and resulted in a very fine and uniform microstructure. Rapid heating depressed the intermediate stages of decomposition resulting in the formation of a nonuniform, coarse structure of alpha, apparently generated via a shear mechanism. The only difference was that the transition between the two precipitation mechanisms occurred at a much slower heating rate due to the generally slower precipitation kinetics.

Aging Response

Microstructure

The aged microstructure was greatly affected by residual deformation substructure if recrystallization was nonuniform such as in the case of low cold reductions.

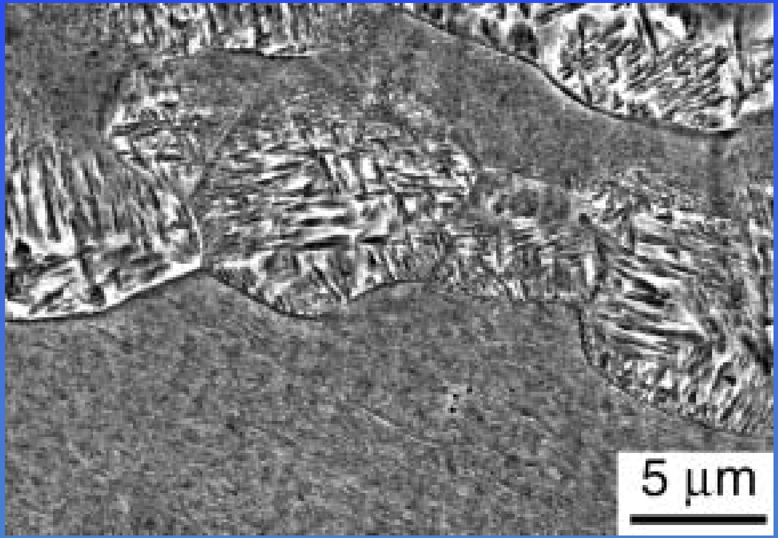

partially recrystallized Ti-15-3 after aging at 538°C for 4 h

Alpha precipitation was markedly different in the recrystallized and the recovered areas. The much finer precipitate structure in recovered regions suggests that continuous heating into the recovery-temperature range may provide a substantially-improved balance of mechanical properties in beta-titanium alloys.

Modulated Structure of Alpha Double-Prime Martensite

NATO Advanced Research Workshop
Metallic Materials with High Structural Efficiency

Strength of Titanium Martensite with Different Crystal Structure

NATO Advanced Research Workshop

Metallic Materials with High Structural Efficiency

Concentrational dependence   Temperature dependence

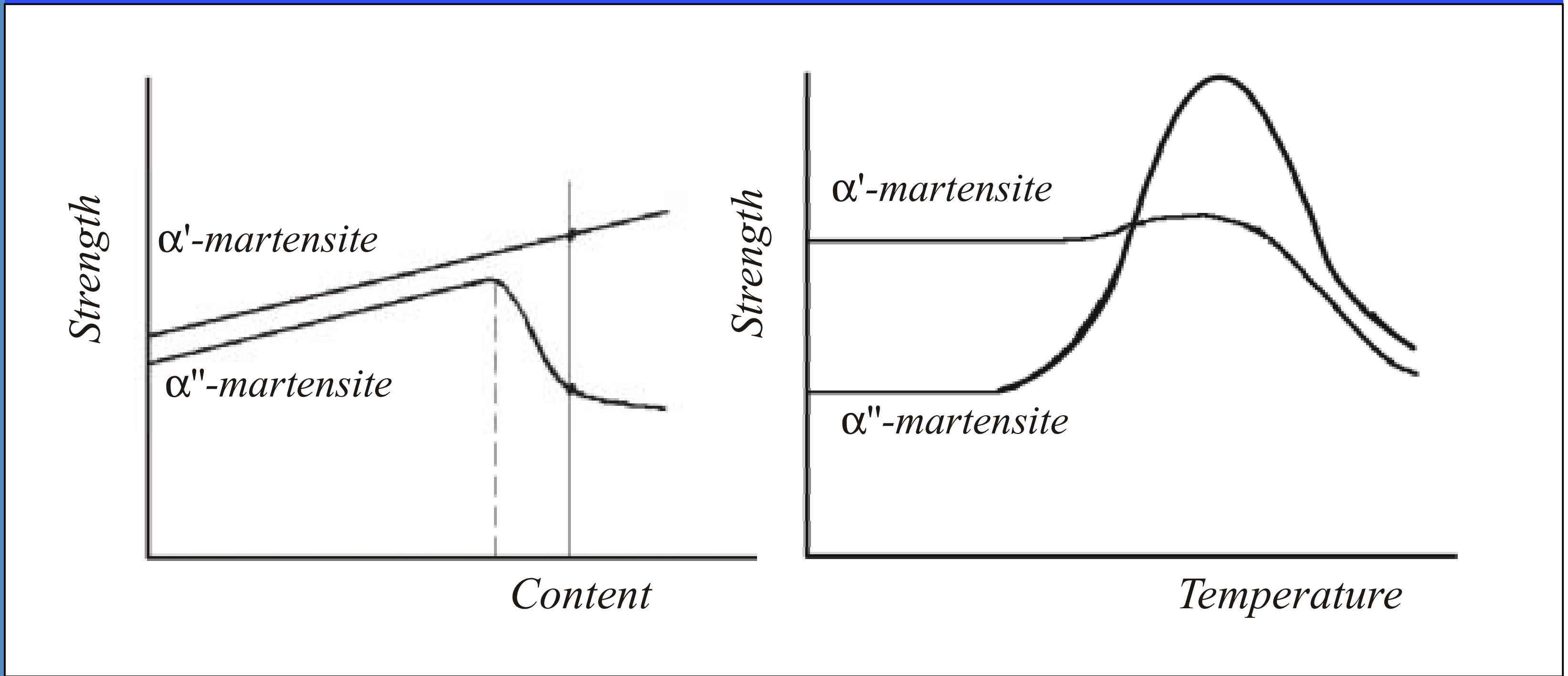

Lattice Parameters of α”-Martensite

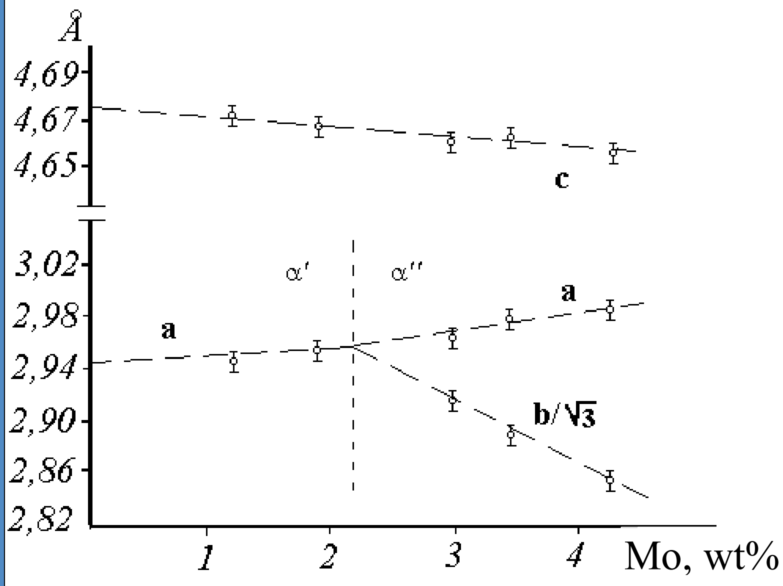

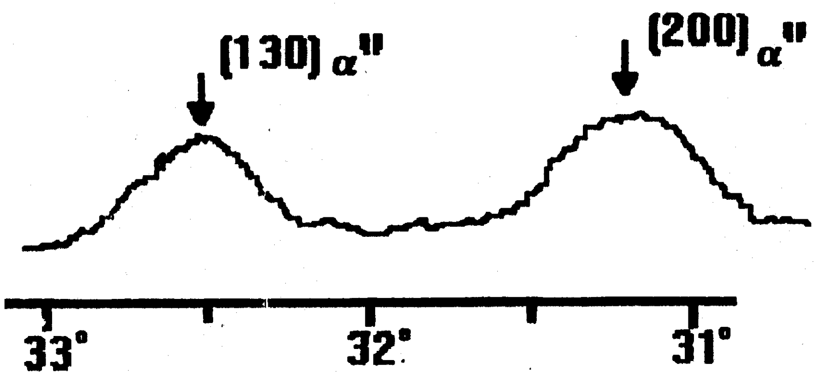

Two Dimensional Modulated Structure in h.c.p. Solid Solution

NATO Advanced Research Workshop

Metallic Materials with High Structural Efficiency

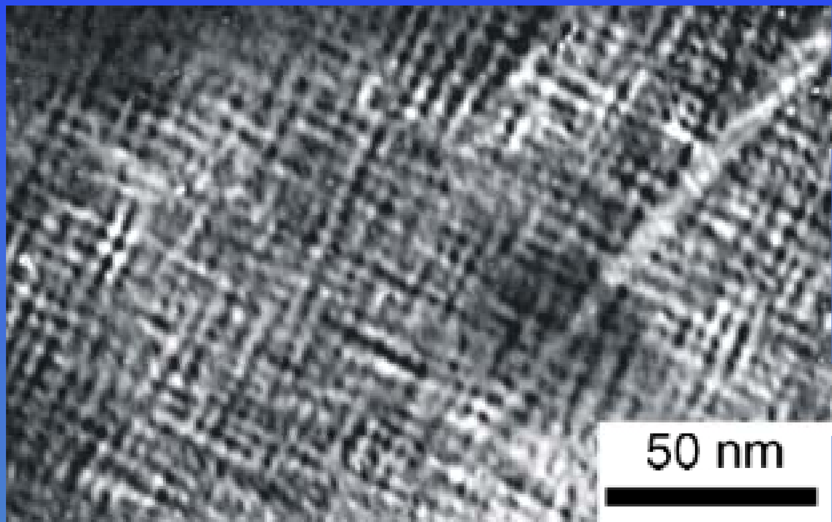

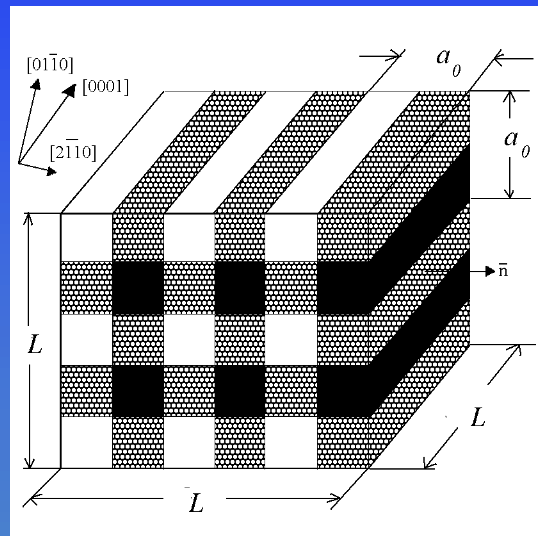

NATO Advanced Research Workshop

Metallic Materials with High Structural Efficiency

Diffraction Effects of Modulated Structure

Deformation under the action of coherent stresses

$$\varepsilon_{ij}(\mathbf{r}) = Ku_0\left[\begin{pmatrix} n_1^2 & n_1n_2 & 0 \\ n_1n_2 & n_2^2 & 0 \\ 0 & 0 & 0 \end{pmatrix} C^{[n_1n_2 0]} + \begin{pmatrix} n_1^2 & -n_1n_2 & 0 \\ -n_1n_2 & n_2^2 & 0 \\ 0 & 0 & 0 \end{pmatrix} C^{[n_1\bar{n}_2 0]}\right]$$

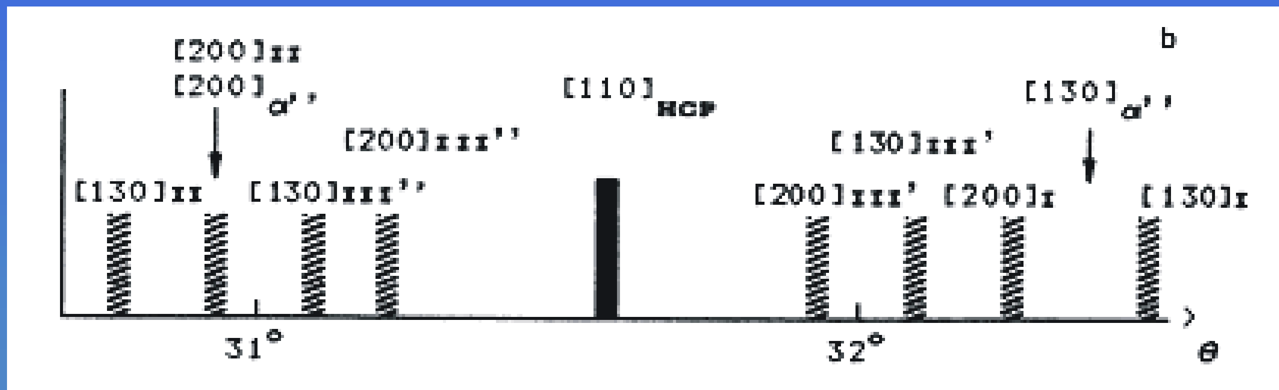

Thermodynamic Analysis of h.c.p. Solid Solutions

Full mixing energy

$$W_{pp'}(\mathbf{r}) \equiv W_{pp'}^{MeMe}(\mathbf{r}) + W_{pp'}^{\mathrm{TiTi}}(\mathbf{r}) - 2W_{pp'}^{Me\mathrm{Ti}}(\mathbf{r})$$

Deformation part

$$\tilde{V}_{pp'}^{MeMe}(\mathbf{k}) \approx -\tilde{F}_{\lambda p}^{i*}(\mathbf{k})\tilde{G}_{ij}^{\lambda\mu}(\mathbf{k})\tilde{F}_{\mu p'}^{j}(\mathbf{k}) + Q_p\delta', \quad (\mathbf{k} \neq \mathbf{0})$$

$$\tilde{V}_{pp'}^{MeMe}(\mathbf{0}) \approx -v_{u.c}\sigma^{pim}L_{p'im} + Q_p\delta_{pp'}$$

Electrochemical part

$$\tilde{\varphi}_{pp'}^{MeMe}(\mathbf{k}) = \sum_{\mathbf{R}} \varphi_{pp'}^{MeMe}(\mathbf{R})\exp(-i\mathbf{k}\cdot\mathbf{R}).$$

$$\varphi_{pp'}^{MeMe}(\mathbf{r}) \approx (A_1A_2\exp(-(b_1+b_2)\mathbf{r}))^{1/2}$$

Fourier Components of Full Mixing Energy

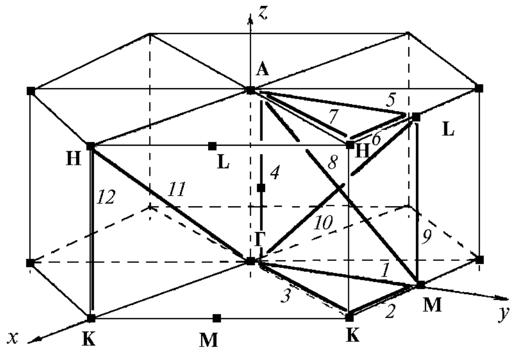

Ti-Fe

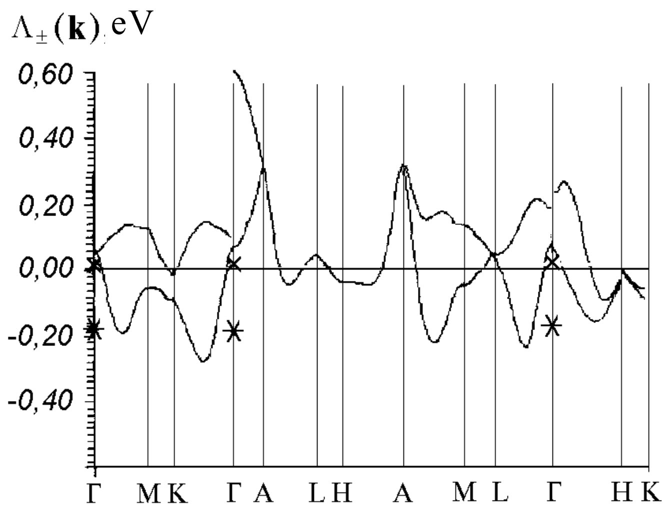

Ti-Mo

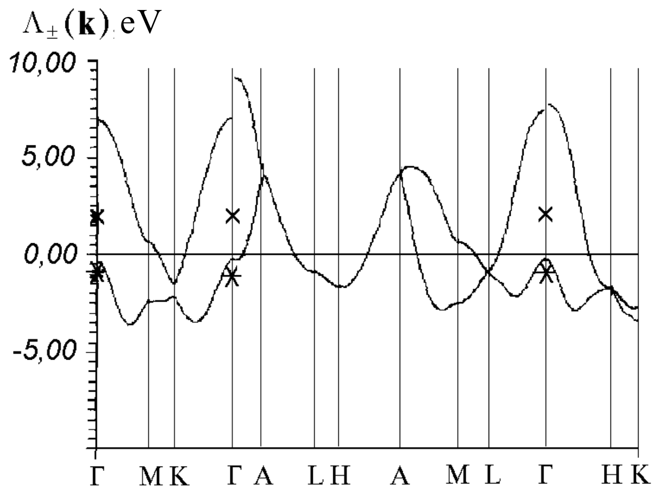

Stability of h.c.p. Solid Solutions

$$b(\mathbf{k},T,c)=\begin{vmatrix}\tilde{V}_{11}(\mathbf{k})+\dfrac{k_bT}{c(1-c)} & \tilde{V}_{12}(\mathbf{k})\\ \tilde{V}^*_{21}(\mathbf{k}) & \tilde{V}_{22}(\mathbf{k})+\dfrac{k_BT}{c(1-c)}\end{vmatrix}\geq 0$$

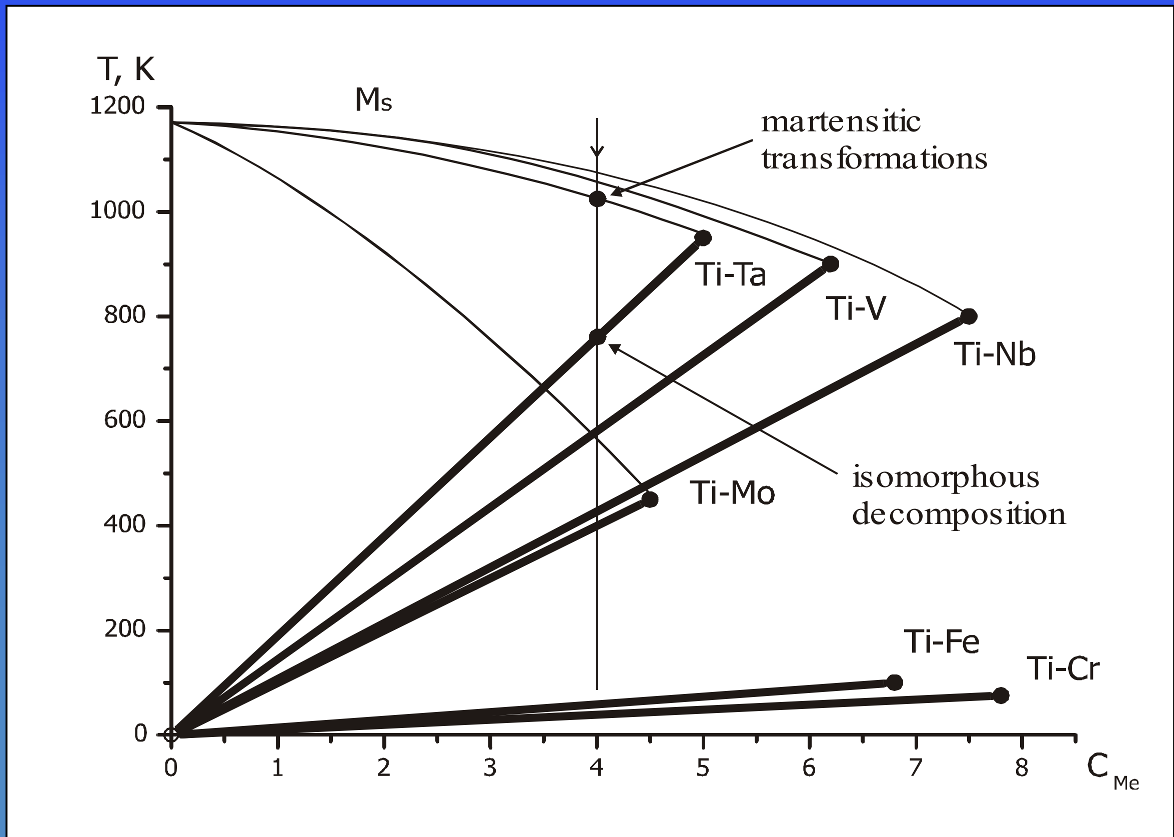

NATO Advanced Research Workshop

Metallic Materials with High Structural Efficiency

Tensile Curves of Modulated Structures

NATO Advanced Research Workshop
Metallic Materials with High Structural Efficiency

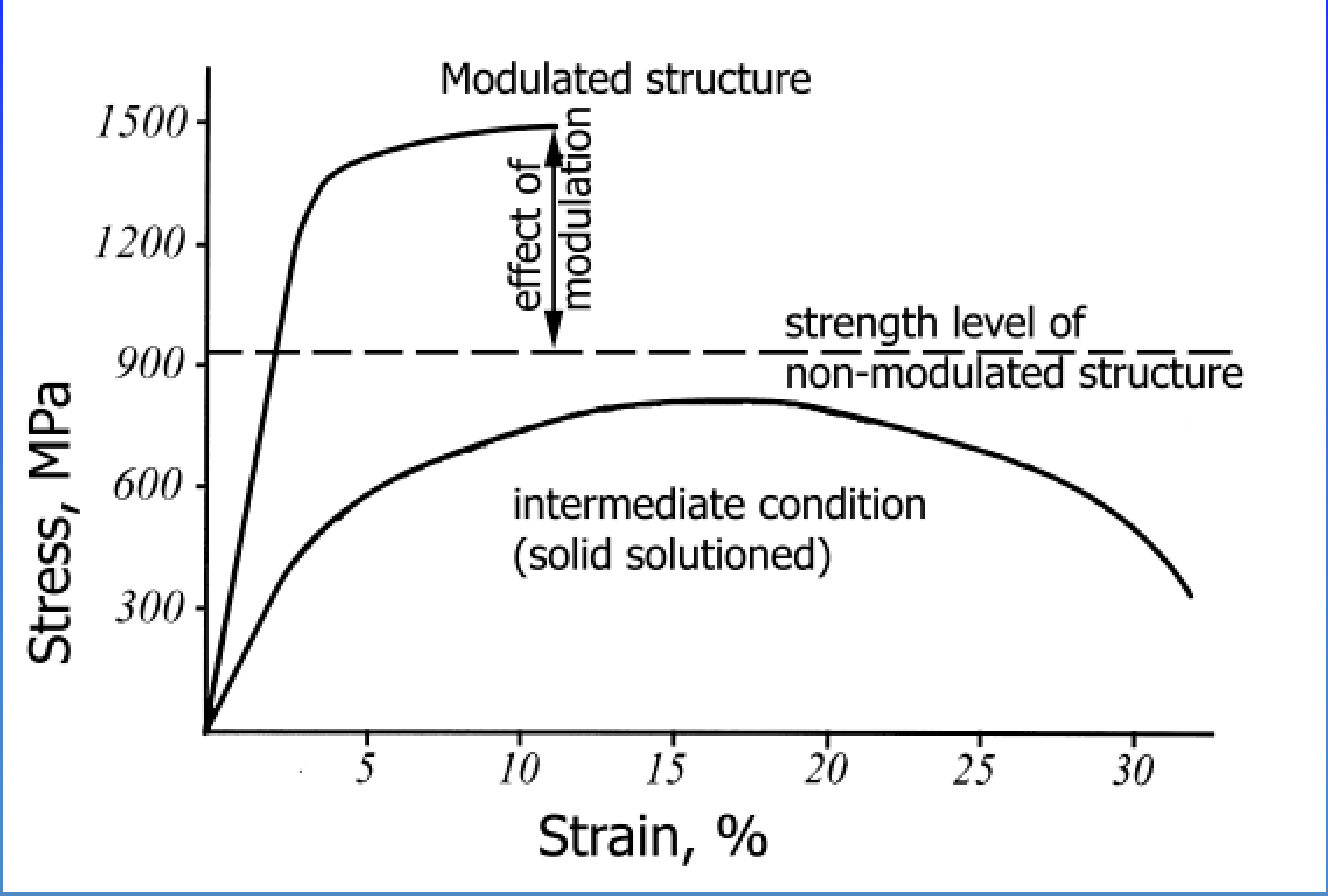

NATO Advanced Research Workshop

Metallic Materials with High Structural Efficiency

Texture Controlled Grain Growth Kinetics at Continuous Heating

Grain Growth upon Continuous Heating

Isothermal conditions:

$$D^n - D_0^n = Kt\exp\left(-Q/RT\right)$$

Continuous heating conditions

$$D^n - D_0^n = \left(KR/\dot{T}Q\right)\left\{\left[T_f^2\exp\left(-Q/RT_f\right)\right]-\left[T_i^2\exp\left(-Q/RT_i\right)\right]\right\}$$

Isotropic condition

Textured condition

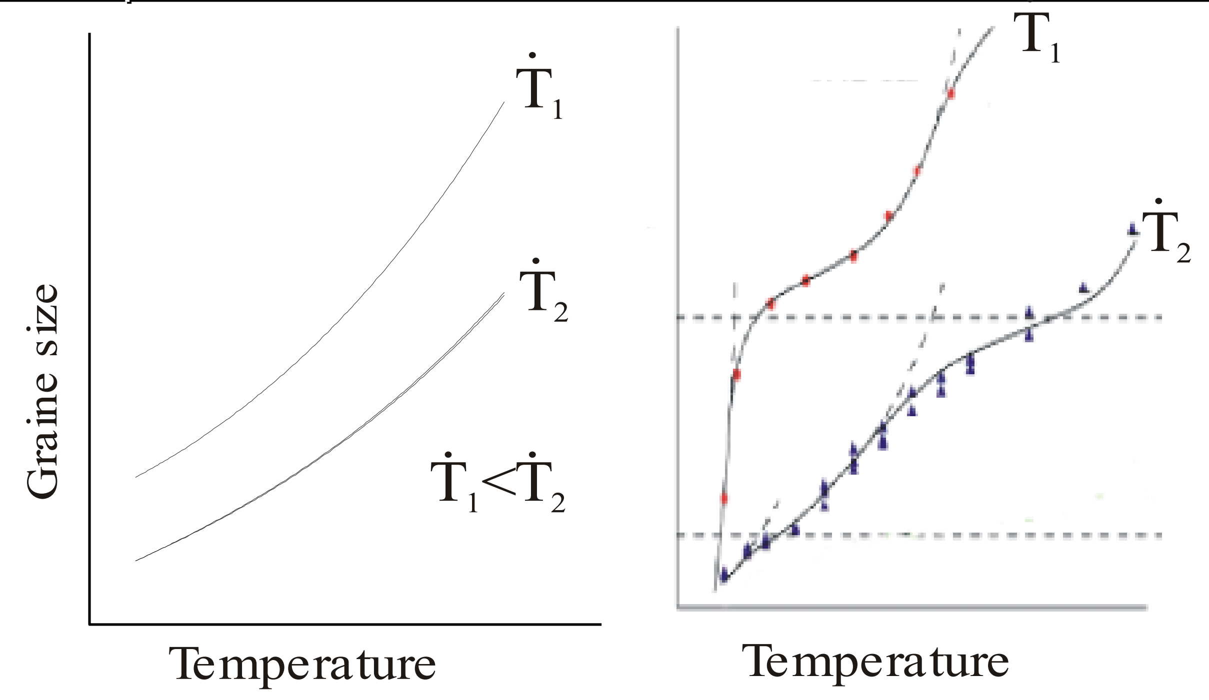

Influence of Texture on Beta Grain Size[1]

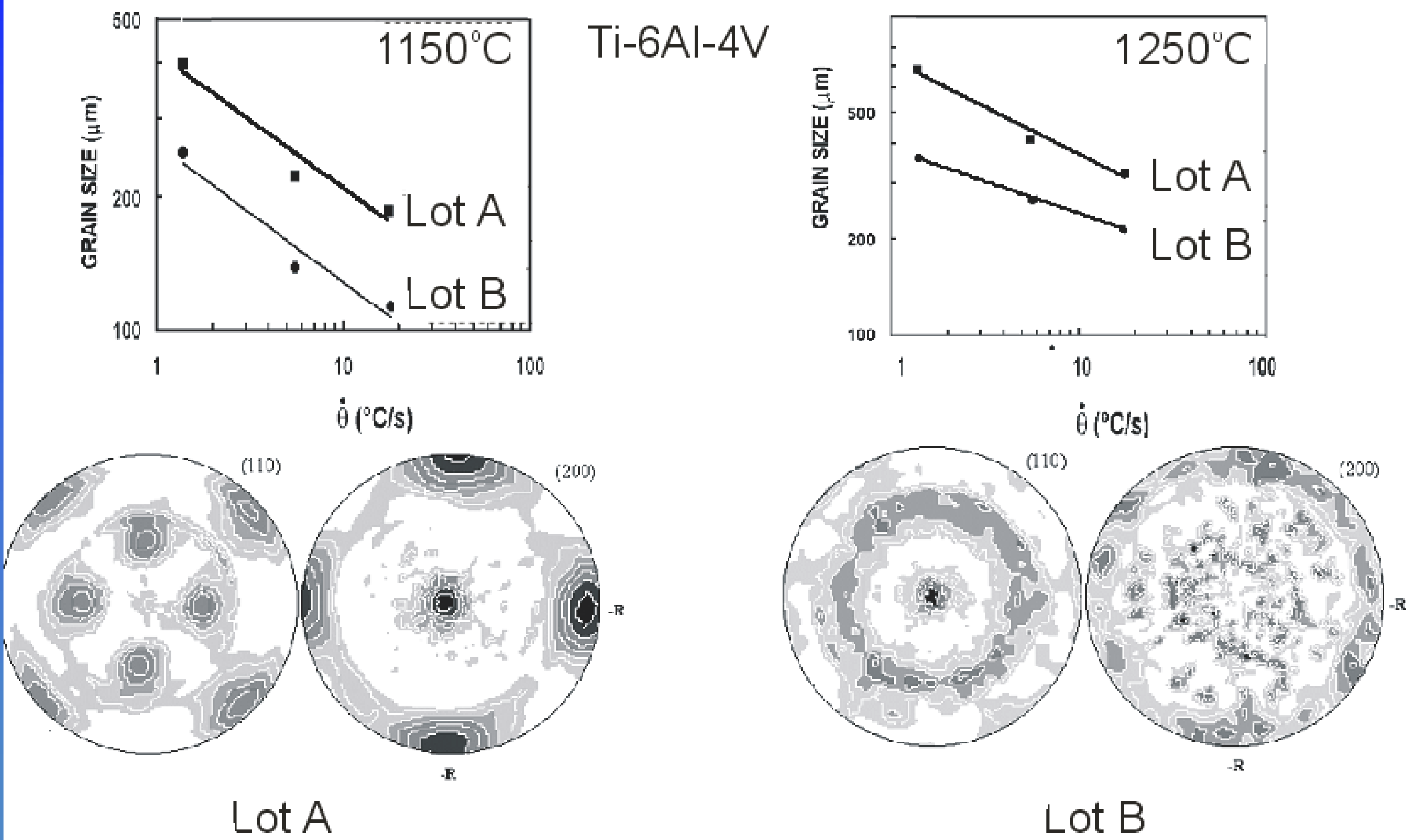

NATO Advanced Research Workshop
Metallic Materials with High Structural Efficiency

[1] S. L. Semiatin, P. N. Fagin, M. G. Glavicic, I. M. Sukonnik, O. M. Ivasishin Mater. Sci. Eng. A299, 2001, 225

Preparation of Starting Materials

Ti-6Al-4V: Ti-6,05Al-4.40V-0.15Fe

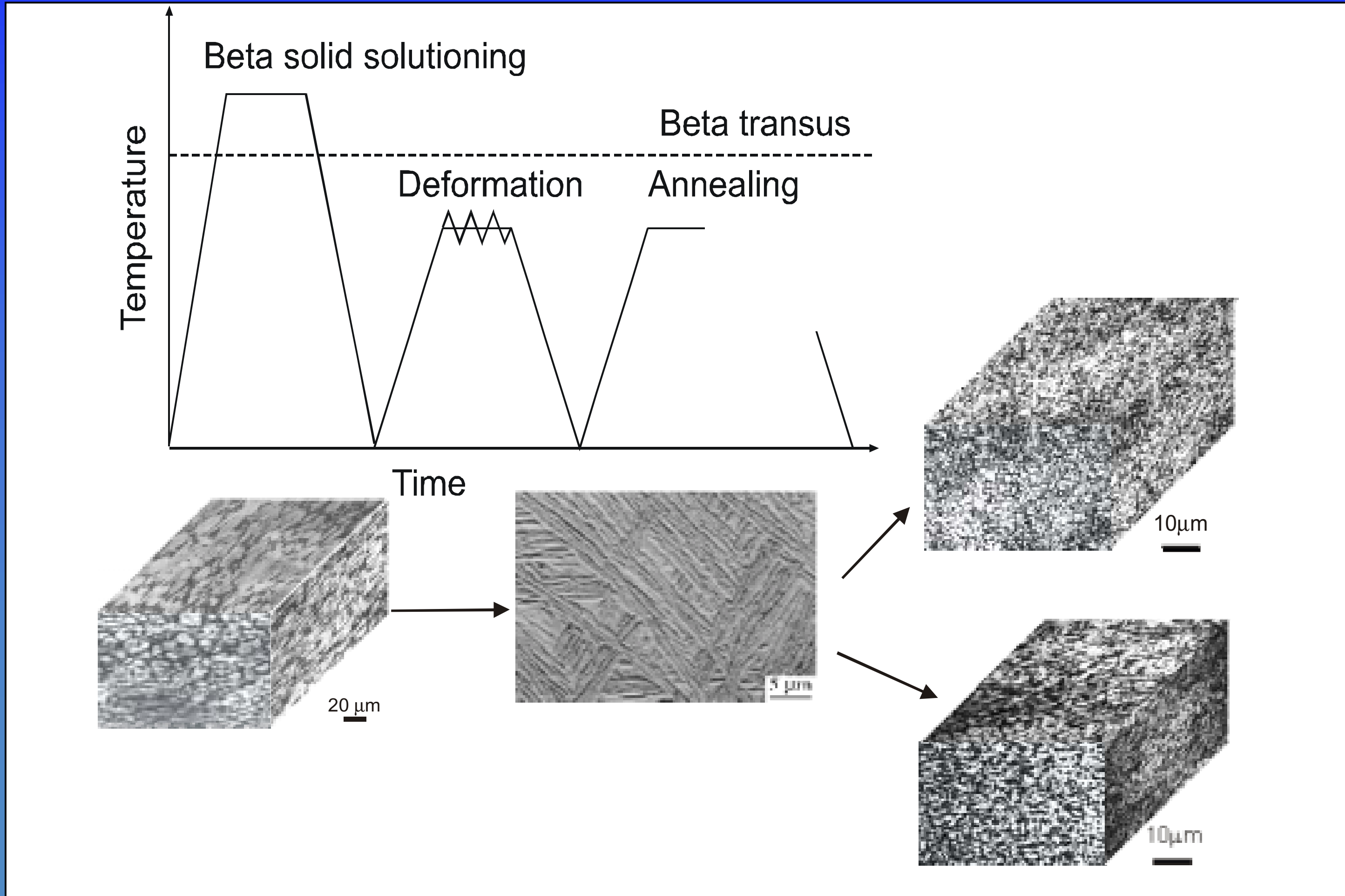

Beta Grain Growth Kinetics for the Ti-6Al-4V Alloy

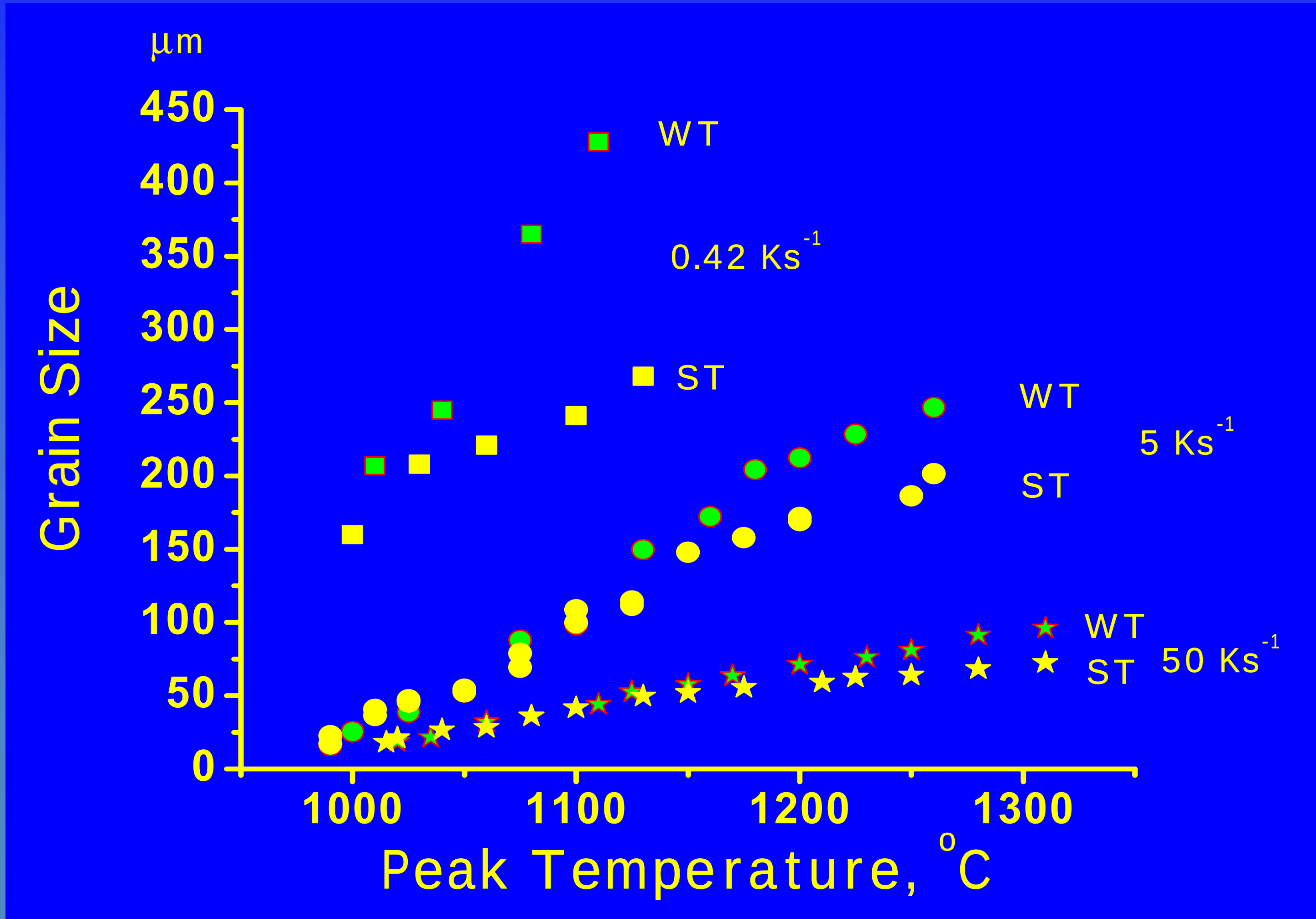

NATO Advanced Research Workshop

Metallic Materials with High Structural Efficiency

NATO Advanced Research Workshop
Metallic Materials with High Structural Efficiency

Beta Grain Growth Kinetics for the VT16 Alloy

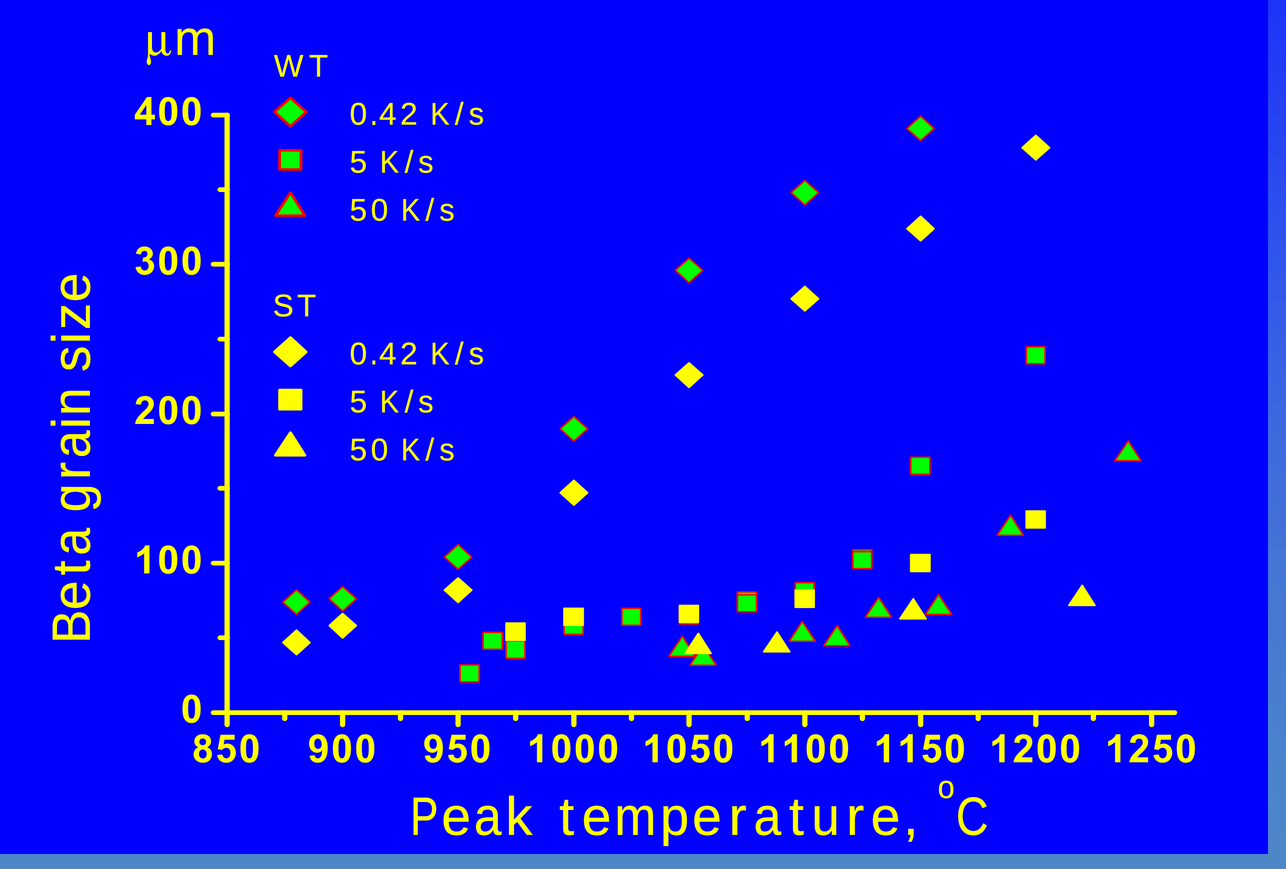

WT – weak textured condition
ST - strong textured condition

Cyclic Texture Evolution in Ti-6Al-4V Alloy Leading to Discontinuous Grain Growth

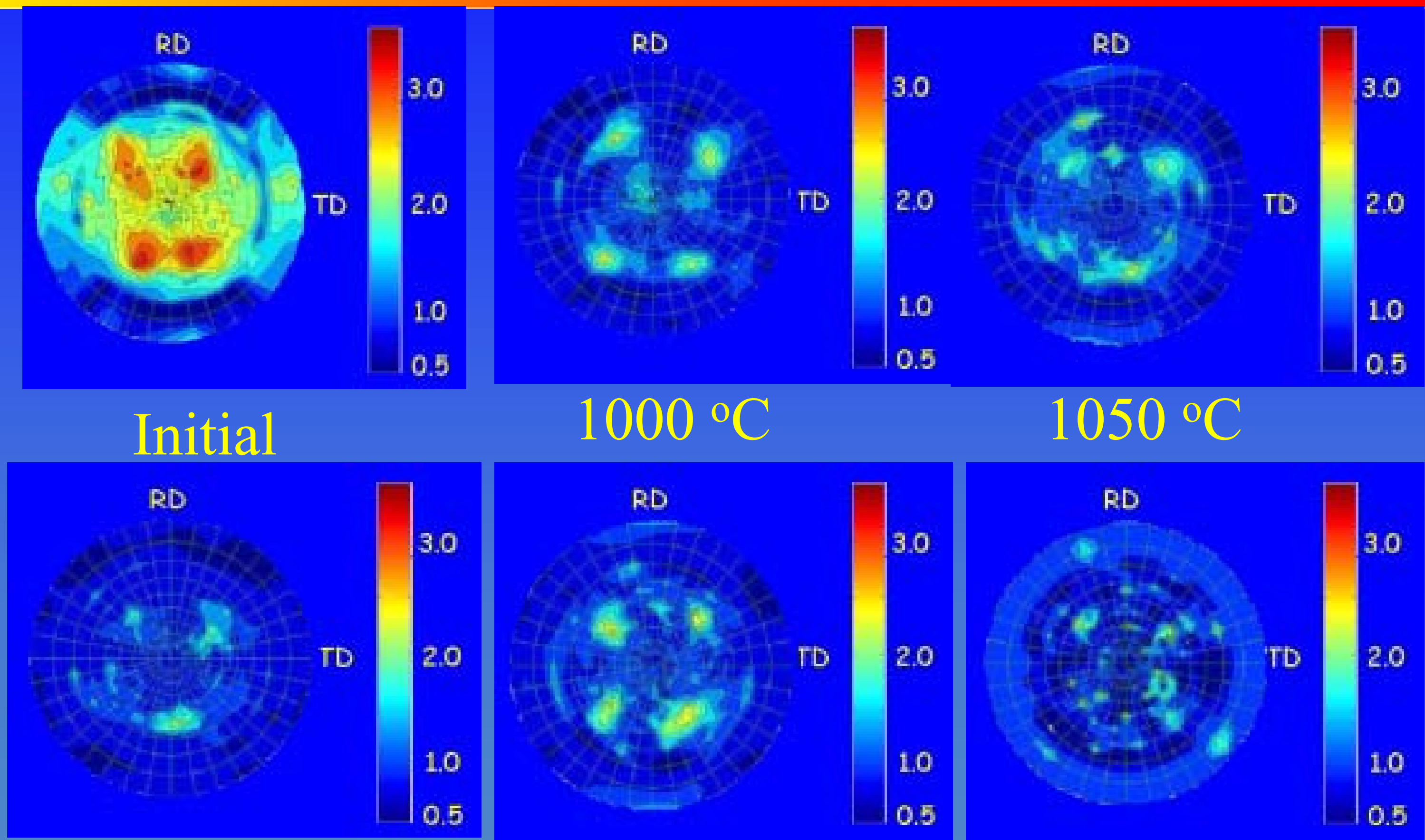

Initial — 1000 °C — 1050 °C

1100 °C — 1150 °C — 1200 °C

During continuous heating, the texture of titanium alloys undergo a cyclic evolution leading to alternating stages of fast and slow grain growth

Typical Beta Grain Growth Behavior Based on Experimental Data

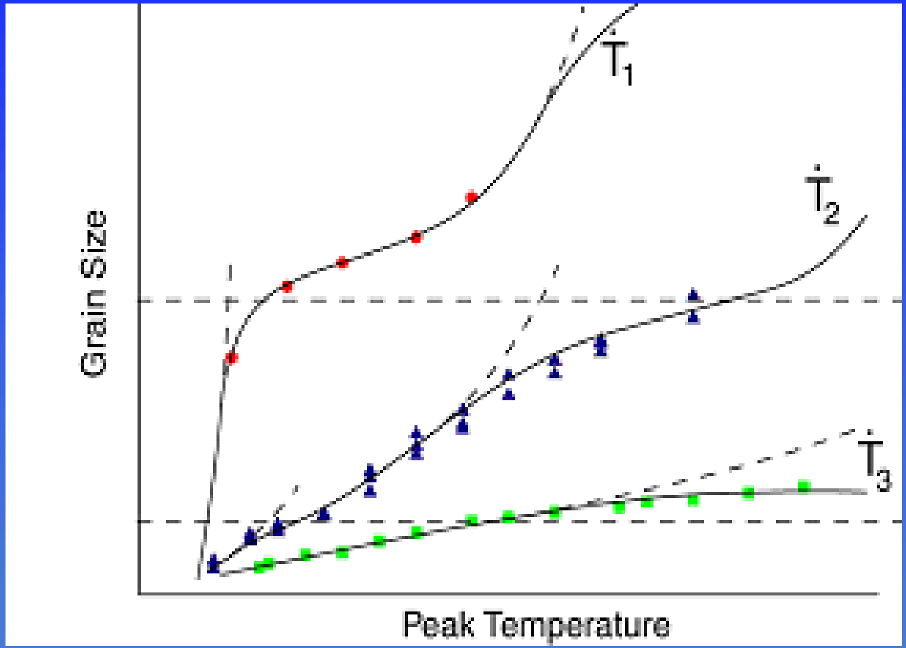

The discontinuous character of grain growth observed for the strong textured material, for which periods of slow and fast grain growth alternates are the result of the periodic texture evolution.

NATO Advanced Research Workshop

Metallic Materials with High Structural Efficiency

Mobility of Boundaries Depending on Texture

Not textured material

Relative GB mobility scale

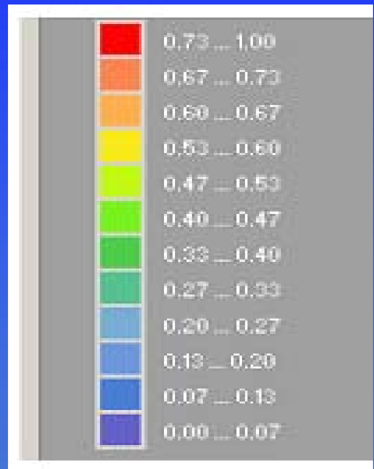

Textured material

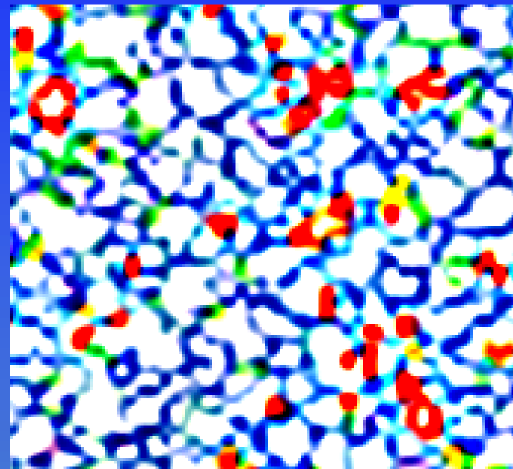

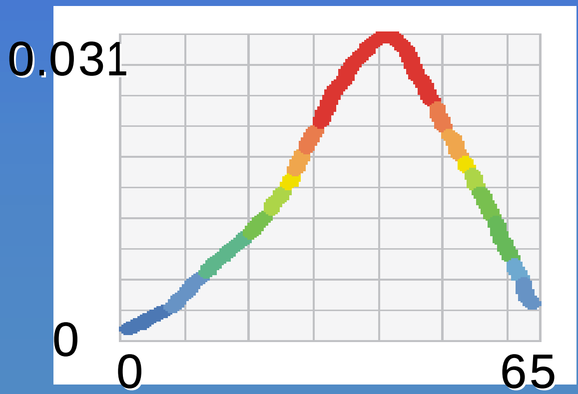

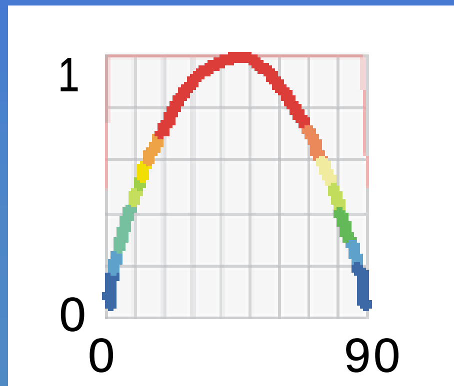

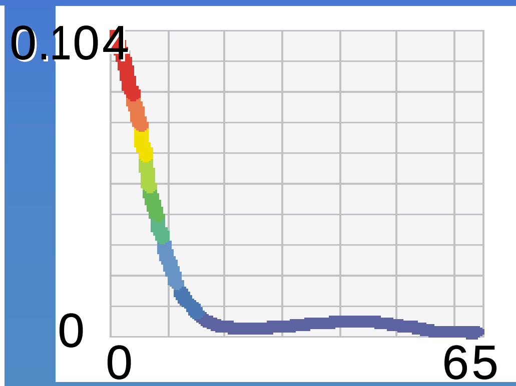

GB distribution functions and GB relative mobility vs. GB misorientation

3D Monte Carlo Simulation of Texture Controlled Grain Growth

NATO Advanced Research Workshop

Metallic Materials with High Structural Efficiency

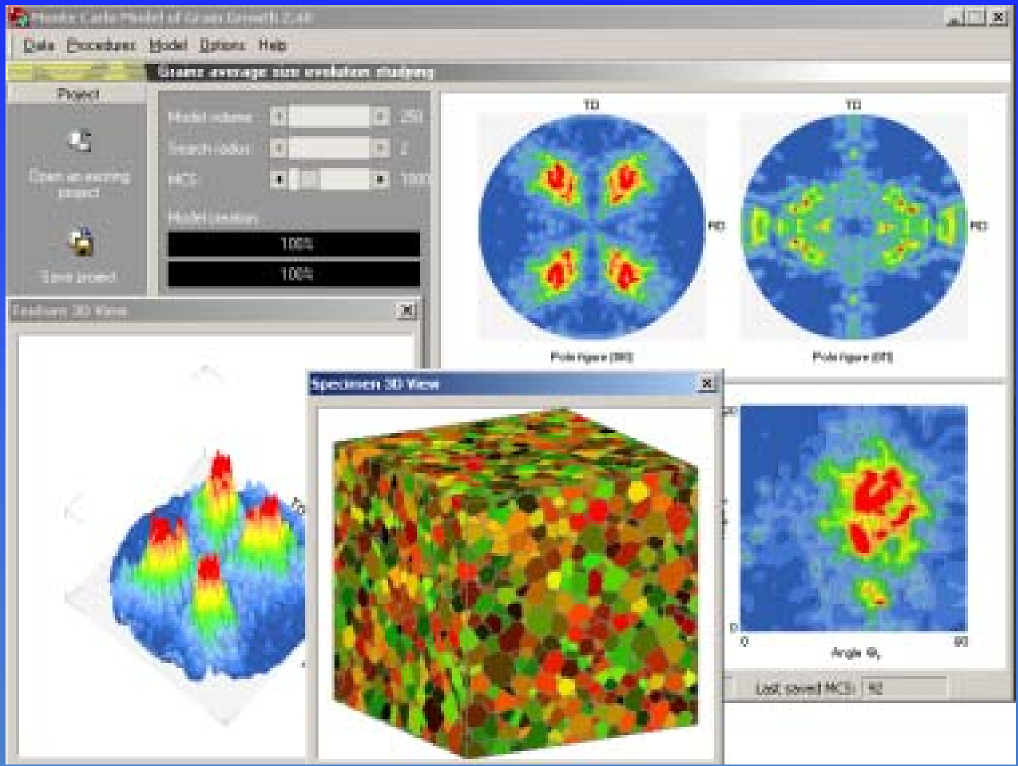

Program complex based on for computationally-efficient 3D Monte-Carlo algorithm was developed to quantify the inter-action of grain growth and texture development during the beta annealing of titanium alloys

Outputs quantified the evolving texture in terms of pole figures or crystallite orientation distribution functions and statistics on the grain structure such as the grain-size distribution and grain boundary misorientation distribution function.

MC Simulation Features

NATO Advanced Research Workshop
Metallic Materials with High Structural Efficiency

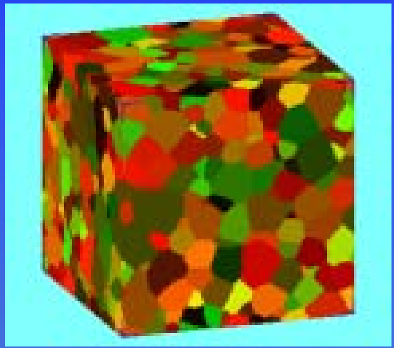

Metropolis orientation flip probability:

$$W = \begin{cases} M_{ij}\exp(-\Delta G / k_b \mathbf{T}); & \Delta G > 0, \\ M_{ij} & \Delta G \le 0, \end{cases}$$

Misorientation dependent GB mobility:

$$M_{ij} = M_0 \ V(g_i, g_j) = M_0 \ V(\varepsilon).$$

MC Simulation Features

NATO Advanced Research Workshop
Metallic Materials with High Structural Efficiency

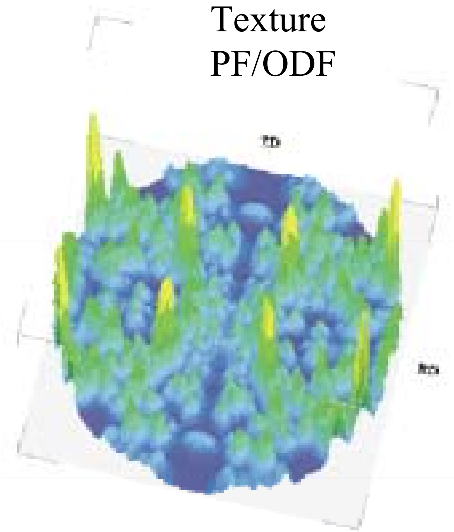

modeling volume 250^3 MUs
up to 200 000 grains
up to 728 000 orientations

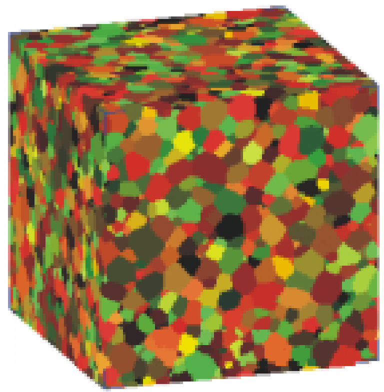

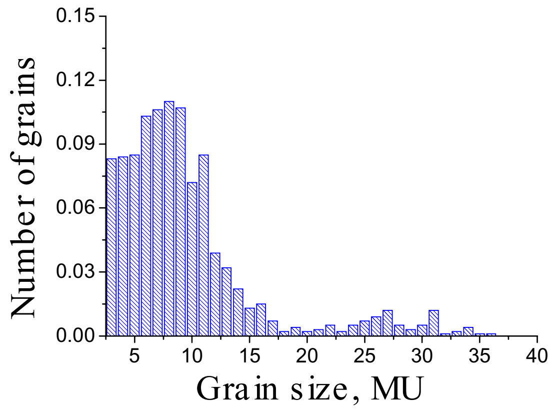

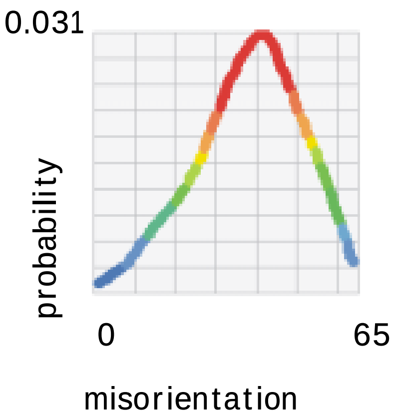

Outputs quantified the evolving texture in terms of pole figures or crystallite orientation distribution functions and statistics on the grain structure such as the grain-size distribution and grain boundary misorientation distribution function.

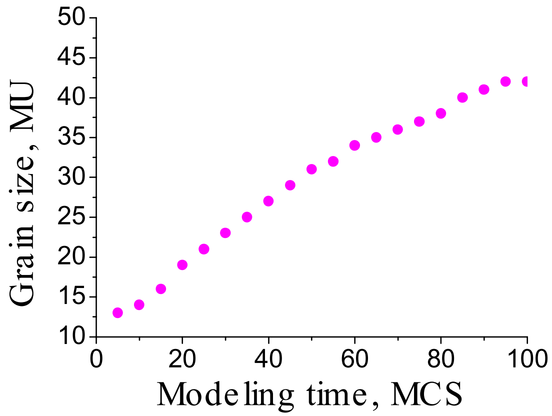

Texture Evolution During Grain Growth – the 3D MC Modeling

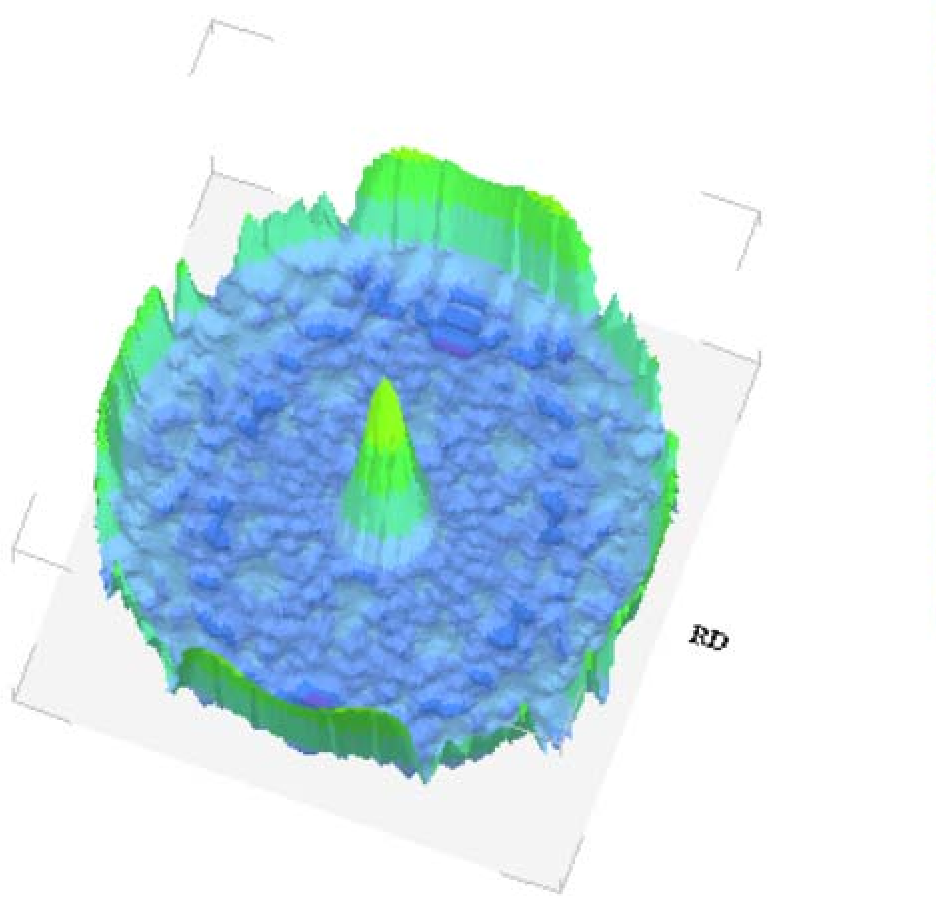

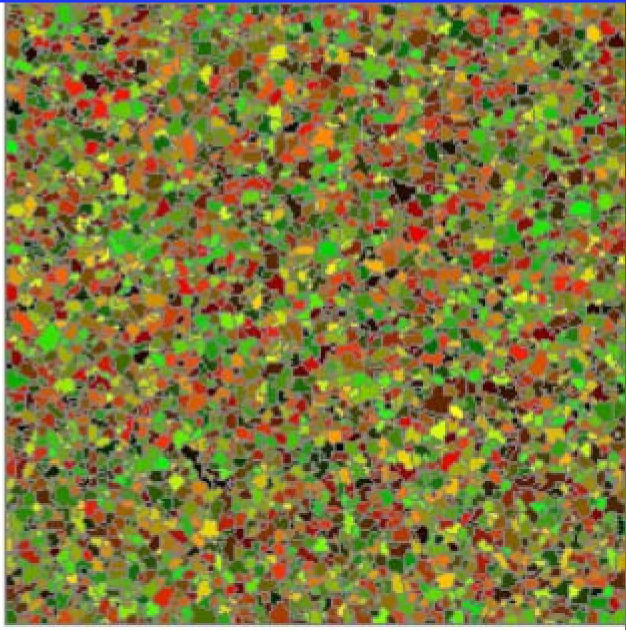

MC Modeling:
Grain Growth Kinetics in Two-Component Textured Material

NATO Advanced Research Workshop

Metallic Materials with High Structural Efficiency

Cyclic texture evolution and volume fraction of the texture component A

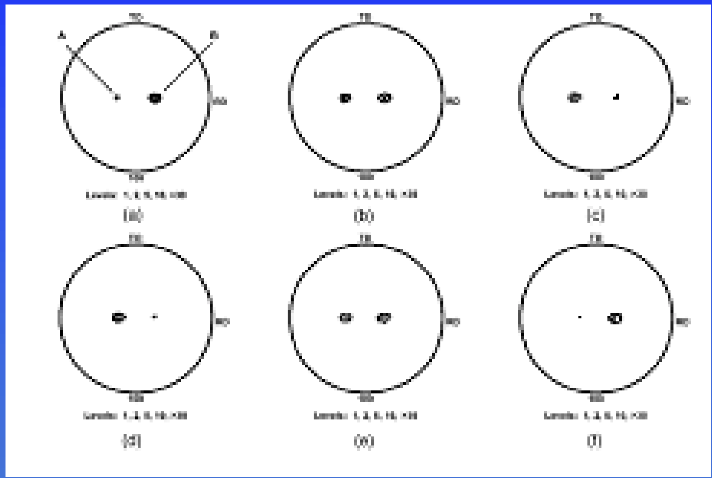

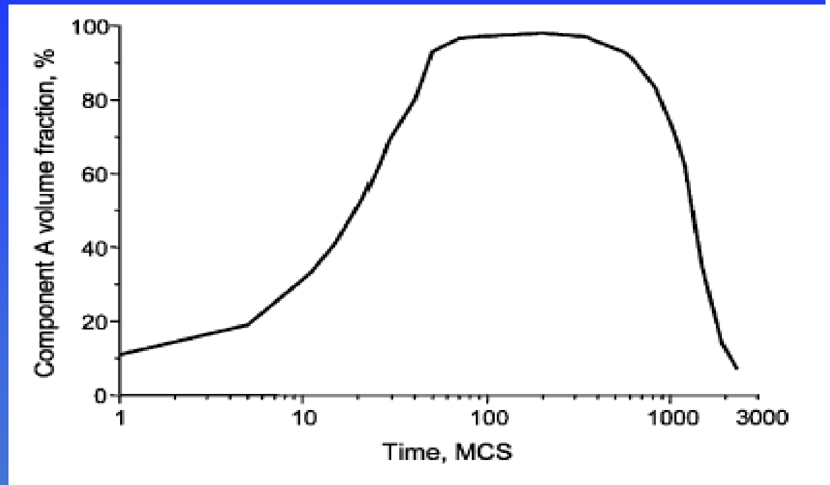

Kinetics of the average grain size in the modeling volume: periods of slow and fast grain growth are the result of the periodic texture evolution

MC Modeling: Abnormal Grain Growth in Heavily Textured Material

Microstructure

GB mobility

Texture

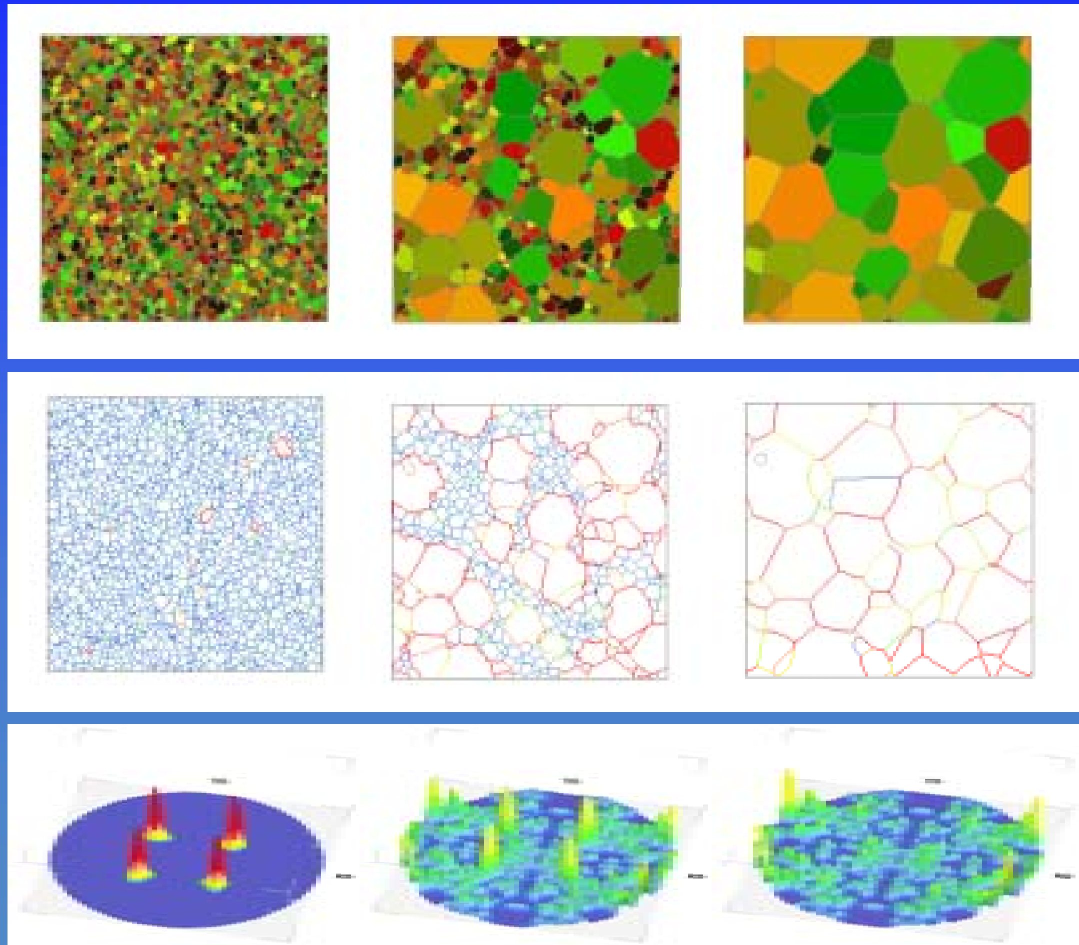

Time, MCS 010 100 250

NATO Advanced Research Workshop
Metallic Materials with High Structural Efficiency

MC Modeling: Application to the Titanium Alloys

Lot A

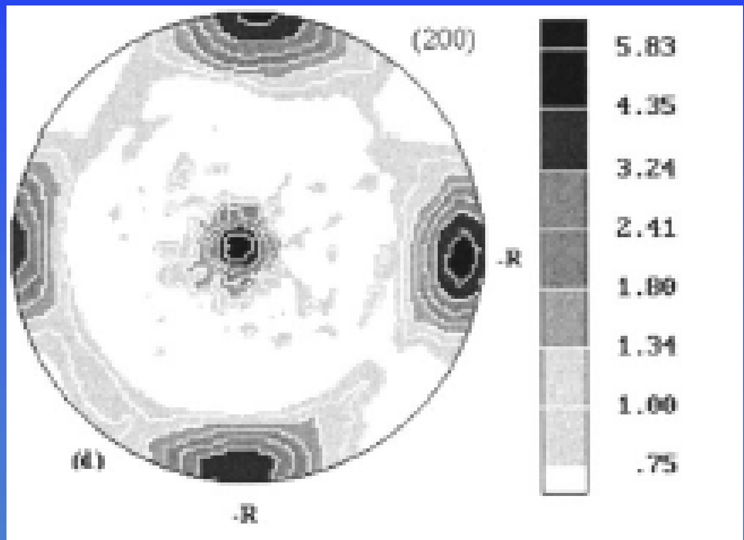

Lot B

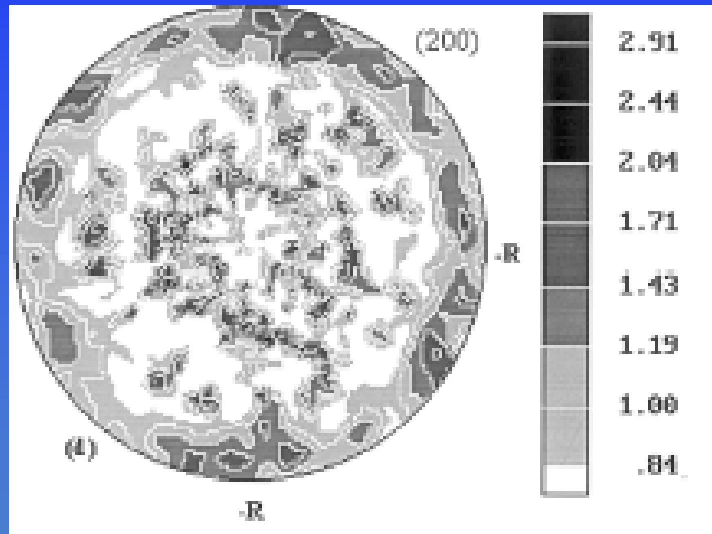

Initial textures[1] of two lots of Ti64 alloy used in simulation

S. L. Semiatin, P. N. Fagin, M. G. Glavicic, I. M. Sukonnik, O. M. Ivasishin
Mater. Sci. Eng. A299, 2001, 225

MC Modeling:
Application to the Titanium Alloys

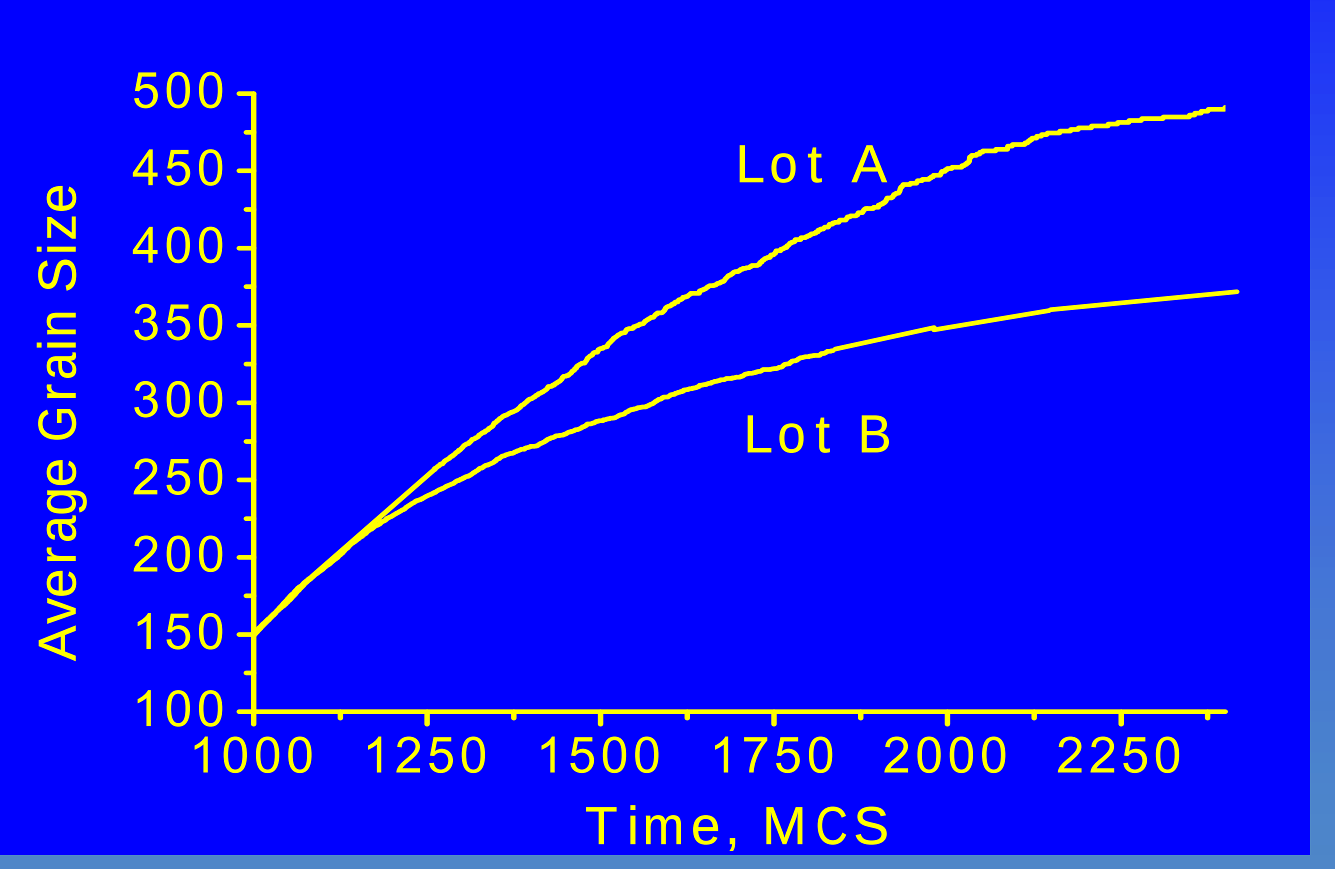

MC simulated grain growth kinetics at isothermal annealing conditions for two lots of Ti64 alloy

NATO Advanced Research Workshop

Metallic Materials with High Structural Efficiency

Conclusions

- Fine-grained fully β-transformed microstructures processed with Rapid Heat Treatment provide an attractive combination of tensile, fatigue, and fracture characteristics of titanium alloys. Main microstructural features favorably influencing the mechanical properties are shorter length of individual alpha plates and shorter length of individual grain boundary.
- Chemical inhomogeneity of high-temperature beta phase allows gradient microstructures to form which, being optimized, exhibit an improved balance of strength and ductility.

Conclusions (continued)

- Additional cold work has proved to be beneficial in further refining the grain structure using rapid recrystallization annealing. Grain sizes of the order of 10 μm and below required to maximize strength whilst maintaining ductility has been received.
- Modulated on nanoscale level structure of a” martensite was explained from thermodynamic point of view. It has proved to be responsible for high level of strength properties.

Conclusions (continued)

- Grain growth during beta annealing of titanium is strongly affected by texture. Periods of rapid and slow growth can be related to the evolution of texture during annealing.

- Many features of such texture-controlled grain growth can be reproduced using an advanced Monte-Carlo (MC) modelling technique that was developed to clarify the interaction of grain growth and texture evolution.

Problems Encountered

Technical:

- special equipment adjusted to sizes is needed

Metallurgical:

- results achieved strongly depend on many parameters of little consequence during conventional thermal processing
- continuous phase and structural transformations need “in-depth” understanding of the effect of heating rate

Acknowledgements

NATO Advanced Research Workshop

Metallic Materials with High Structural Efficiency

The present work was supported by the Air Force Office of Scientific Research (AFOSR) and the AFOSR European Office of Aerospace Research and Development (AFOSR/EOARD) within the framework of STCU partner projects P-041 and P-057. The encouragement of the AFOSR program managers (Drs. C.S. Hartley, R. Fredell (P-041) and C.H. Ward (P-057)) is greatly appreciated.